

A Shapley Value Estimation Speedup for Efficient Explainable Quantum AI

IAIN BURGE*, SAMOVAR, Télécom SudParis, Institut Polytechnique de Paris, 91120 Palaiseau, France

MICHEL BARBEAU†, School of Computer Science, Carleton University, Canada

JOAQUIN GARCIA-ALFARO*, SAMOVAR, Télécom SudParis, Institut Polytechnique de Paris, 91120 Palaiseau, France

This work focuses on developing efficient post-hoc explanations for quantum AI algorithms. In classical contexts, the cooperative game theory concept of the Shapley value adapts naturally to post-hoc explanations, where it can be used to identify which factors are important in an AI's decision-making process. An interesting question is how to translate Shapley values to the quantum setting and whether quantum effects could be used to accelerate their calculation. We propose quantum algorithms that can extract Shapley values within some confidence interval. Our method is capable of quadratically outperforming classical Monte Carlo approaches to approximating Shapley values up to polylogarithmic factors in various circumstances. We demonstrate the validity of our approach empirically with specific voting games and provide rigorous proofs of performance for general cooperative games.

CCS Concepts: • **Applied computing** → **Physics**; • **Hardware** → **Quantum computation**; • **Computing methodologies** → **Machine learning algorithms**; • **Theory of computation** → **Algorithmic game theory**.

Additional Key Words and Phrases: Shapley Value, Quantum Computing, Cooperative Game Theory, Explainable Quantum Machine Learning, Machine Learning, Artificial Intelligence, Quantum Machine Learning.

ACM Reference Format:

Iain Burge, Michel Barbeau, and Joaquin Garcia-Alfaro. 2025. A Shapley Value Estimation Speedup for Efficient Explainable Quantum AI. 1, 1 (April 2025), 34 pages. <https://doi.org/10.1145/1122445.1122456>

1 INTRODUCTION

As Artificial Intelligence (AI) becomes a larger part of critical decision-making processes, it is important to understand the logic behind the decisions being made. Transparency in AI has become a topic of substantial regulatory importance worldwide. In the European Union, the General Data Protection Regulation (GDPR) provides citizens the right to explanations for impactful automated decisions which relate to personal data [1]. More recently, in 2024, the European Union enacted the AI act. The AI act provides individuals, in the context of high-risk AI systems, the right to an explanation for: (i) the use of an AI system in the decision-making process; (ii) the most important elements of that decision [2]. In the United States, the *Maintaining American Leadership in AI* executive order tasked the National Institute of Standards and Technology (NIST) with developing a plan for robust and safe research and development in AI [3]. NIST's plan listed explainability as an aspect of trustability, which is one of their key areas of focus. This wave

Authors' addresses: Iain Burge, iain-james.burge@telecom-sudparis.eu, SAMOVAR, Télécom SudParis, Institut Polytechnique de Paris, 91120 Palaiseau, France; Michel Barbeau, barbeau@scs.carleton.ca, School of Computer Science, Carleton University, 1125 Col. By Dr., Ottawa, Ontario, Canada, K1S 5B6; Joaquin Garcia-Alfaro, joaquin.garcia_alfaro@telecom-sudparis.eu, SAMOVAR, Télécom SudParis, Institut Polytechnique de Paris, 19 place Marguerite Perey, Palaiseau, 91120 Palaiseau, France.

Permission to make digital or hard copies of all or part of this work for personal or classroom use is granted without fee provided that copies are not made or distributed for profit or commercial advantage and that copies bear this notice and the full citation on the first page. Copyrights for components of this work owned by others than ACM must be honored. Abstracting with credit is permitted. To copy otherwise, or republish, to post on servers or to redistribute to lists, requires prior specific permission and/or a fee. Request permissions from permissions@acm.org.

© 2025 Association for Computing Machinery.

of legislative attention poses a substantial challenge, as many of today’s state-of-the-art AI algorithms, such as deep learning models, are unexplainable black boxes [4]. Without specialized tools, AI developers often cannot understand the reasoning of their models. There are several paths one can take to satisfy the new need for model explanations, the most popular approach is to create post hoc explanations for black-box models. Post hoc explanations have the advantage that we can continue to use powerful black box models, such as computer vision models, without being entirely blind to their inner workings.

This paper¹ focuses on additive explanations, which indicate inputs with the largest effect on a particular output [6]. For example, if one were to apply for a bank loan and be rejected, an additive explanation would quantify the impact of features such as income, location, and debt on the application’s rejection. When applied to AI models, these explanations describe which inputs are most important in making a particular decision. Several methods have been proposed for generating additive explanations; however, only one satisfies the important properties of local accuracy, missingness, and consistency [6]. This method is based on the Shapley value, a solution concept from cooperative game theory often used in economic game theory.

In game theory, the Shapley value is a weighted average of the contribution provided by a player to every possible coalition of other players. To apply Shapley values to the analysis of AI models, we simply consider each feature a player and interpret a player being included or excluded from a coalition as a feature being on or off. Unfortunately, the direct calculation of Shapley values is NP-Hard. This means it takes an exponential number of operations [7, 8]. Outside of some special cases, random sampling is the only option for approximation [9].

In parallel to the growth in AI, we have seen an emergence of quantum computation and quantum AI [10]. Due to the fickle nature of quantum information, the problem of explainability is amplified since measuring a quantum system destroys information. As a result, many quantum algorithms act as ultra-black boxes, where their internal workings are impossible to comprehend or even fully measure. Though the field of eXplainable Quantum AI (XQAI) is still emerging, there exists some work into finding the Shapley values of quantum algorithms [11, 12], and a bit into other additive methods such as LIME [13]. Existing methods for Shapley-based explanations either rely on knowing the algorithm’s structure as a quantum circuit or random sampling. By Chebyshev’s inequality, random sampling is quadratic in complexity, twice the precision is four times the work [14]. Fortunately, it is often possible to do better in by leveraging quantum effects.

In this paper, we detail an efficient algorithm for calculating the Shapley values of the input qubits of a quantum circuit. In some cases, our method provides a quadratic speedup, up to polylogarithmic factors, when compared to Monte-Carlo methods. With a fixed likelihood for success and a fixed range of outputs, we can have an arbitrarily accurate Shapley value approximation where the quantum query complexity grows inversely to precision.

The paper is organized as follows. Section 2 provides background and preliminaries on Shapley values. Section 3 is composed of Subsection 3.1, which introduces a guiding example problem, and Subsection 3.2, which provides a simple example of Shapley Values use in explainability. Sections 4 and 5 present our algorithms. The error and complexity analysis are covered in Appendix D. Section 6 demonstrates the application of our methods to the problem discussed in section 3. Section 7 provides an improved version of our quantum algorithm for Shapley value approximation. Section 8 surveys related work. Section 9 concludes the article.

¹The work presented in this paper extends early research [5].

2 BACKGROUND

This section presents preliminaries on Shapley values, including the notation used, as defined in Table 1, and formal definitions.

Table 1. Notation and symbols used in this section

$G = (F, V)$: Coalitional game, F being a set of players and V a function which assigns a value to each subset of players (Definition 1)
$\Phi(G, i), \Phi(i)$: Player i 's payoff, or Shapley value, which represents how important they are in the game G (Definitions 2, 3)
$\Phi^\pm(i)$: $\Phi^-(i)$ is a weighted average of the value of each subset not including player i (Definition 3) : $\Phi^+(i)$ is a weighted average of the value of each subset including player i (Definition 3) : The difference $\Phi^+(i) - \Phi^-(i)$ is equal to the i th player's Shapley value $\Phi(i)$ (Definition 3)
V^\pm	: V^- is the value of a subset excluding player i (Definition 3) : V^+ is the value of a subset including player i (Definition 3)
$\gamma(n, m)$: The weights used to calculate $\Phi^\pm(i)$ (Definition 3)

Cooperative game theory is the study of coalitional games. In this article, we are most interested in Shapley values. We now list some definitions and preliminaries,

DEFINITION 1 (COALITIONAL GAME). A coalitional game is a tuple $G = (F, V)$. $F = \{0, 1, \dots, n\}$ is a set of $n + 1$ players. $V : \mathcal{P}(F) \rightarrow \mathbb{R}$ is a value function with $V(S) \in \mathbb{R}$ representing the value of a given coalition $S \subseteq F$, with the restriction that $V(\emptyset) = 0$.

DEFINITION 2 (PAYOFF VECTOR). Given a game $G = (F, V)$, there exists a payoff vector $\Phi(G)$ of length $n + 1$. Each element $\Phi(G, i) \in \mathbb{R}$ represents the utility of player $i \in F$. The value function determines a payoff vector. Player i 's payoff value $\Phi(G, i)$ is determined by how $V(S)$, $S \subseteq F$, is affected by i 's inclusion or exclusion from S .

There are a variety of solution concepts for constructing payoffs [15]. We focus on the Shapley solution concept, which returns a payoff vector [16]. Each element of the payoff vector $\Phi(G, i)$, is called player i 's Shapley value. Shapley values have various interpretations depending on the game being analyzed.

Shapley values are derived using one of several sets of axioms. We use the following four [16]. Suppose we have games $G = (F, V)$ and $G' = (F, V')$, and a payoff vector $\Phi(G)$, then:

- (1) Efficiency: The sum of all utility is equal to that of the grand coalition (the coalition containing all players),

$$\sum_{i=0}^n \Phi(G, i) = V(F).$$

- (2) Equal Treatment: Players i, j are said to be symmetrical if for all $S \subseteq F$, where $i, j \notin S$ we have that $V(S \cup \{i\}) = V(S \cup \{j\})$. If i and j are symmetric in G , then they are treated equally, $\Phi(G, i) = \Phi(G, j)$.

- (3) Null Player: Consider a player $i \in F$, if for all $S \subseteq F$ such that $i \notin S$, we have $V(S) = V(S \cup \{i\})$, then i is a null player. If i is a null player, then $\Phi(G, i) = 0$.

- (4) Additivity: If a player is in two games G and G' , then the Shapley values of the two games are additive

$$\Phi(G + G', i) = \Phi(G, i) + \Phi(G', i)$$

where a game $G + G'$ is defined as $(F, V + V')$, and $(V + V')(S) = V(S) + V'(S)$, $S \subseteq F$.

These axioms lead to a single unique and intuitive division of utility [16]. The values of the payoff vectors can be interpreted as the responsibility of the respective players for the final outcome [17]. When player i has a small payoff $\Phi(G, i)$, then player i has a neutral impact on the final outcome. When player i has a large payoff, then player i greatly impacts the final outcome.

DEFINITION 3 (SHAPLEY VALUE [18]). *Let $G = (F, V)$, for notational simplicity, we write $\Phi(G, i)$ as $\Phi(i)$. The Shapley value of the i^{th} player is,*

$$\Phi(i) = \Phi^+(i) - \Phi^-(i), \quad (1)$$

where,

$$\Phi^+(i) = \sum_{S \subseteq F \setminus \{i\}} \gamma(|F \setminus \{i\}|, |S|) V^+(S), \quad V^+(S) = V(S \cup \{i\}), \text{ and}, \quad (2)$$

$$\Phi^-(i) = \sum_{S \subseteq F \setminus \{i\}} \gamma(|F \setminus \{i\}|, |S|) V^-(S), \quad V^-(S) = V(S). \quad (3)$$

Given $n = |F \setminus \{i\}|$,

$$\gamma(n, m) = \frac{1}{\binom{n}{m}(n+1)}.$$

REMARK 1. *The Shapley value is equivalently written as,*

$$\Phi(i) = \sum_{S \subseteq F \setminus \{i\}} \gamma(|F \setminus \{i\}|, |S|) (V(S \cup \{i\}) - V(S)).$$

The Shapley value of i is the expected marginal contribution to a random coalition $S \subseteq F \setminus \{i\}$, where the marginal contribution is equal to $V(S \cup \{i\}) - V(S)$ [17]. Each player's Shapley value can be interpreted as a weighted average of their contributions. Where the weights, $\gamma(n, m)$, have an intuitive interpretation: the factor $1/\binom{n}{m}$ results in each possible size of S having an equal impact on the final value. Since, given $|S| = m$, there would be $\binom{n}{m}$ summands contributing to the final value. The multiplicand $1/(n+1)$ averages between the different sizes of S .

LEMMA 1. *We have that $\sum_{S \subseteq F \setminus \{i\}} \gamma(|F \setminus \{i\}|, |S|)$ is equal to one.*

PROOF. Let us define $H_m = \{S \in \mathcal{P}(F \setminus \{i\}) : |S| = m\}$. We can rewrite $\sum_{S \subseteq F \setminus \{i\}} \gamma(|F \setminus \{i\}|, |S|)$ as,

$$\sum_{m=0}^n \sum_{S \in H_m} \gamma(n, m).$$

Plugging in the definition for γ ,

$$\sum_{m=0}^n \sum_{S \in H_m} \frac{1}{\binom{n}{m}(n+1)} = \frac{1}{n+1} \sum_{m=0}^n \frac{1}{\binom{n}{m}} \sum_{S \in H_m} 1.$$

Since there are n choose m possible subsets of size m and hence n choose m possible subsets in H_m , it follows that we have,

$$\frac{1}{n+1} \sum_{m=0}^n \frac{1}{\binom{n}{m}} \binom{n}{m}.$$

Hence, the result holds. ■

We develop algorithms for general games and demonstrate them for a monotonic game.

DEFINITION 4 (MONOTONIC GAME). *A game is monotonic if for all $S, H \subseteq F$, we have, $V(S \cup H) \geq V(S)$. Note that when a game is monotonic, every summand in Equation (1) is non-negative.*

A naive approach to finding the i^{th} player's Shapley value is through direct calculation using the Shapley Equation (1), completing the task in $O(2^n)$ assessments of V . For structured games, it may be possible to calculate Shapley values more efficiently. Otherwise, another option is random sampling [9]. Substantial trade-offs exist in each case. We propose a quantum algorithm with some substantial advantages in the following sections.

3 CLASSICAL SHAPLEY VALUE APPLICATIONS

3.1 Weighted Voting Games

Let us model a player's voting power as a weighted count of instances in which the player has the deciding vote. The Shapley values correspond to voting power. Three friends sit around a table. They are deliberating a grave matter. Should they get Chinese food for the second weekend in a row? They decide to take a vote. Alice just got a promotion at work. To celebrate this, their friends agreed to give them three votes. Bob, the youngest of the group, also had good news, an incredible mark on their latest assignment! Everyone decided Bob should get two votes. Charley, who had nothing to celebrate, and who is generally disliked, gets one vote. The group decides to go out for Chinese food if there are four *yes* votes. In the end, all the friends vote for Chinese food.

At the restaurant, they run into their friend David, a mathematician. David is intrigued when they hear about their vote. David begins to wonder how much power each friend had in the vote. The intuitive answer is that Alice had the most voting power, Bob had the second most, and Charley had the least. However, David notices something strange. Bob does not seem to have a more meaningful influence than Charley. There are no cases where Bob's two votes would do more than Charley's single vote. David concludes, there must be a more nuanced answer. David heard of cooperative game theory and Shapley values. David might be able to answer the question.

How can Definition 3 be applied to David's problem? Consider the game $G = (F, V)$. The players are Alice (0), Bob (1), and Charley (2) represented as the set $F = \{0, 1, 2\}$. Denote each player's voting weight as $w_0 = 3$, $w_1 = 2$, and $w_2 = 1$. Recall that the vote threshold is q equal to four. Then, for any subset $S \subseteq F$, we can define V as:

$$V(S) = \begin{cases} 1 & \text{if } \sum_{j \in S} w_j \geq q, \\ 0 & \text{otherwise.} \end{cases} \quad (4)$$

$V(S)$ is one when the sum of players' votes in S reaches the threshold of four. Otherwise, the vote fails and $V(S)$ is zero. This is called a weighted voting game [7]. One could easily add more players with arbitrary non-negative weights and thresholds. Note that weighted voting games fall into the family of monotonic games (Definition 4).

In this context, the terms in the Shapley value equation have an intuitive meaning. Take player i , and consider a set $S \subseteq F \setminus \{i\}$. If $V(S \cup \{i\}) - V(S) = 1$, then the i^{th} player is a deciding vote for the set of players S . Otherwise, player i is not a deciding vote.

Thus, for weighted voting games, player i 's Shapley value represents a weighted count of how many times i is a deciding vote. We can work out the Shapley values by hand, noting that,

$$\begin{aligned} V(\emptyset) &= 0, & V(\{0\}) &= 0, & V(\{1\}) &= 0, & V(\{0, 1\}) &= 1, \\ V(\{2\}) &= 0, & V(\{0, 2\}) &= 1, & V(\{1, 2\}) &= 0, & V(\{0, 1, 2\}) &= 1 \end{aligned}$$

From this, we have:

$$\begin{aligned}
\Phi(0) &= \sum_{S \subseteq F \setminus \{i\}} \gamma(|F \setminus \{i\}|, |S|) \cdot (V(S \cup \{i\}) - V(S)) \\
&= \gamma(2, 0) \cdot (V(\{0\}) - V(\emptyset)) + \gamma(2, 1) \cdot (V(\{0, 1\}) - V(\{1\})) \\
&\quad + \gamma(2, 1) \cdot (V(\{0, 2\}) - V(\{2\})) + \gamma(2, 2) \cdot (V(\{0, 1, 2\}) - V(\{1, 2\})) \\
&= 2 \cdot \gamma(2, 1) + \gamma(2, 2) = \frac{2}{3}
\end{aligned}$$

This can be repeated to get $\Phi(1)$ and $\Phi(2)$ equal to $1/6$.

In the case of Alice, Bob, and Charley's voting game, it is trivial to calculate their respective Shapley values. However, what if one hundred colleagues were choosing a venue for a party, all with different numbers of votes? In that case, a direct calculation would take 2^{100} assessments of V ! For this more general case, we need to be clever.

3.2 Explainability and Shapley Values of Binary Classifiers

Explainable AI can be broken into two categories, inherent explainability, and post-hoc explainability [4]. Inherently explainable models rely on algorithms which are easy to interpret, such as small decision trees or linear models. Ideally, every application would use inherently explainable models [4]; however, contemporary models tend to be black boxes which are very large and non-linear, e.g., deep neural networks. As a result, post-hoc methods, which attempt to explain black box decisions, have become an important form of harm-reduction. A promising research direction looks at using counterfactuals, questions of the form “*what is the smallest change that can be made to the input to change the output*,” as explanations [19, 20]. This paper focuses primarily on additive explanations, which assign importance to each input of a model [6].

There are multiple approaches to producing model explanations, one of the most promising being based on Shapley Values [6]. We introduce a simplified but rigorous method to leverage Shapley Values for explainability. Suppose we have a binary classifier $C : \{0, 1\}^{r \times r} \rightarrow \{0, 1\}$, which classifies binary strings of length r^2 . This could, for example, represent a classifier which takes a r by r black and white medical scan and decides whether a patient has a cancerous tumour [21]. This is easily translated to a cooperative game. We consider each input bit (respectively pixel) to be a player in $F = \{0, \dots, r^2 - 1\}$. Each binary string $h = h_{r^2-1} \dots h_1 h_0 \in \{0, 1\}^{r \times r}$ represents a coalition S_h where player j is included if and only if h_j is one (or equivalently, the j th pixel is white),

$$S_h = \{j : h_j = 1, j \in \mathbb{Z}_r\}.$$

We can then define our value function $V_C : \mathcal{P}(F) \rightarrow \mathbb{R}$ to correspond to the classifier C ,

$$V_C(S_h) = C(h_{r^2-1} \dots h_1 h_0).$$

Using this change in perspective we can now leverage tools from cooperative game theory. In particular, we can now assign each input bit h_j an importance, its Shapley value Φ_j . For our tumour classifier example, this would give us a heat map of where the classifier focuses on the most when it makes decisions. This represents a global explanation, which gives a general idea of which features (a.k.a., players or pixels) are most important for decision-making generally.

We can also define a method which gives local explanations. This gives an idea of which features were most important for a particular decision. Suppose we want to understand why classifier decided that $C(x) = y$, where $x = x_{r^2-1} \dots x_1 x_0 \in \{0, 1\}^{r \times r}$ and $y \in \{0, 1\}$. We define a new value function, as follows:

$$V_{C,x}(S_h) = \frac{1}{2^{|F \setminus S_h|}} \sum_{Q \subseteq F \setminus S_h} |V_C(S_x) - V_C((S_x \cap S_h) \cup Q)|. \quad (5)$$

For a given set $Q \subseteq F \setminus S_h$, player $k \in F$ is in $(S_x \cap S_h) \cup Q$ if either: $k \in Q$ which implies $k \notin S_h$; or if $k \in S_h$ and S_x . In more simple terms, when k is in S_h , its inclusion in $(S_x \cap S_h) \cup Q$ is based on its inclusion in S_x , otherwise, it is based on its inclusion in Q . We average the change in classification across every possible $Q \subseteq F \setminus S_h$. In effect, our value function fixes a subset of features S_h in x , and every feature in $F \setminus S_h$ is replaced with noise. The Shapley values derived from $V_{C,x}$ describe the importance of features in the decision of $C(x) = y$. Note that local explanations could be described differently, but this particular definition is highly compatible with the quantum algorithm described in the following sections.

4 QUANTUM ALGORITHM FOR SHAPLEY VALUE APPROXIMATION

Table 2. Notation and symbols used in sections 4, 5 and 7

V_{\max}, V_{\min}	: Maximum and minimum coalition values in the range of V , Equations (6), (7)
S_h	: Set of players encoded by integer h 's binary representation (Definition 5)
$V^\pm(h)$: Normalized value of S_h for V^- , and of $S_h \cup \{i\}$ for V^+ , Equations (8), (9)
B^\pm	: Operation taking h and encoding a scaled $\hat{V}^\pm(h)$ in the amplitude of an output bit, Eq. (10)
$ x _H$: Hamming distance from 0 of integer x 's binary representation, Equation (11)
$ \mu^\pm\rangle$: Quantum state encoding $\Phi^\pm(i)$ in the expected value of measuring the final bit, Equation (12)
Player Register	: Player register P1 stores a superposition of all possible player coalitions
Utility Register	: Value of each coalition is encoded in the amplitudes of the utility register Ut qubit

We represent the Shapley value calculation problem in the quantum context. Consider an $n + 1$ player game G represented by the pair (F, V) , where $F = \{0, 1, \dots, n\}$ and $V : \mathcal{P}(F) \rightarrow \mathbb{R}$, with $V(\emptyset) = 0$. Table 2 gives an overview for the notation in this and the next section (Sections 4 and 5). We define V_{\max} as an upper bound and V_{\min} as the lower bound of the value function,

$$V_{\max} \geq \max_{S \subseteq F} V(S), \text{ and,} \quad (6)$$

$$V_{\min} \leq \min_{S \subseteq F} V(S). \quad (7)$$

The goal is to implement a quantum version of $V(S)$ and apply it on a superposition representing all possible subsets $S \subseteq F \setminus \{i\}$ and $S \cup \{i\}$. We first define two quantum registers, the player and utility registers. The player register P1 represents player coalitions and requires n qubits. Meanwhile, the utility Ut register requires one qubit, and in its probability amplitude, represents the output of V given a player coalition.

DEFINITION 5. *To encode coalitions in the player register, consider the selection binary sequence $h = h_n \dots h_{i+1} h_{i-1} \dots h_0 \in \{0, 1\}^n$. Let S_h be the set of all players $j \in F$ such that $h_j = 1$. S_h can represent any player coalition that excludes the player i given the corresponding h .*

In the player register, the computational basis states represent different subsets of players, where the j th qubit represents the j th player. In this encoding, the j th qubit being $|1\rangle$ represents j 's inclusion in the subset. $|0\rangle$ represents its exclusion. Thus, every possible subset of players excluding player i has a corresponding basis state. It follows that representing every subset of players simultaneously in a quantum superposition is possible. The one-qubit utility register encodes the output of V .

Next, we define a function that maps V to the interval $[0, 1]$,

$$\hat{V}^\pm(h) := \frac{V^\pm(S_h) - V_{\min}}{V_{\max} - V_{\min}}, \quad (8)$$

where,

$$V^+(h) := \frac{V(S_h \cup \{i\}) - V_{\min}}{V_{\max} - V_{\min}} \quad \text{and} \quad V^-(h) := \frac{V(S_h) - V_{\min}}{V_{\max} - V_{\min}}. \quad (9)$$

We define the following 2^{n+1} by 2^{n+1} block diagonal matrix:

$$B^\pm = \bigoplus_{h=0}^{2^n-1} \begin{pmatrix} \sqrt{1 - \gamma(n, |h|_H) \cdot \hat{V}^\pm(h)} & \sqrt{\gamma(n, |h|_H) \cdot \hat{V}^\pm(h)} \\ \sqrt{\gamma(n, |h|_H) \cdot \hat{V}^\pm(h)} & -\sqrt{1 - \gamma(n, |h|_H) \cdot \hat{V}^\pm(h)} \end{pmatrix}, \quad (10)$$

where $|h|_H$ is the Hamming distance between h and 0 in n bits, or the number of ones in the binary representation of h . Formally, if $x = x_{n-1} \cdots x_0 \in \{0, 1\}^n$, then,

$$|x|_H := |\{j : x_j = 1, j \in \{0, \dots, n-1\}\}| \quad (11)$$

As a result, $|h|_H$ is the number of players in the coalition S_h .

THEOREM 1. *The block diagonal matrix $B^\pm(n)$ is unitary.*

PROOF. It follows from the fact that each block

$$\begin{pmatrix} \sqrt{1 - \gamma(n, |h|_H) \cdot \hat{V}^\pm(h)} & \sqrt{\gamma(n, |h|_H) \cdot \hat{V}^\pm(h)} \\ \sqrt{\gamma(n, |h|_H) \cdot \hat{V}^\pm(h)} & -\sqrt{1 - \gamma(n, |h|_H) \cdot \hat{V}^\pm(h)} \end{pmatrix}$$

of B^\pm is unitary. ■

We construct the quantum system:

$$|\mu^\pm\rangle = B^\pm(H^{\otimes n} \otimes I) |0\rangle_{P1}^{\otimes n} |0\rangle_{Ut}. \quad (12)$$

where $|0\rangle_{P1}^{\otimes n}$ represents the player register, and $|0\rangle_{Ut}$ represents the utility register in their initial states.

THEOREM 2. *The expected value of the utility register of system $|\mu^+\rangle$ minus the expected value of the utility register of system $|\mu^-\rangle$ is,*

$$\frac{\Phi(i)}{2^n(V_{\max} - V_{\min})}.$$

PROOF. It follows from the fact that

$$(H^{\otimes n} \otimes I) |0\rangle_{P1} |0\rangle_{Ut} = \sum_{h=0}^{2^n-1} \frac{1}{\sqrt{2^n}} |h\rangle_{P1} |0\rangle_{Ut}$$

and the following sequence of equivalences, where $B_{k+1,k}$ is the element of B at row $k+1$ column k :

$$\begin{aligned} \sum_{h=0}^{2^n-1} (B_{h+1,h})^2 &= \sum_{h=0}^{2^n-1} \phi(h, n) = \sum_{h=0}^{2^n-1} \gamma(n, |h|_H) \cdot \hat{V}^\pm(h) \\ &= \sum_{S \subseteq F \setminus \{i\}} \gamma(|F \setminus \{i\}|, |S|) \cdot \left(\frac{V^\pm(S) - V_{\min}}{V_{\max} - V_{\min}} \right) \end{aligned}$$

Hence, the probability of measuring a one in the utility register of the quantum system $|\mu^\pm\rangle$ is

$$\frac{1}{2^n \cdot (V_{\max} - V_{\min})} \left(-V_{\min} + \sum_{S \subseteq F \setminus \{i\}} \gamma(|F \setminus \{i\}|, |S|) \cdot V^\pm(S) \right)$$

Thus, the expected value of $\langle \mu^+ | (I^{\otimes n} \otimes |1\rangle\langle 1|) | \mu^+ \rangle - \langle \mu^- | (I^{\otimes n} \otimes |1\rangle\langle 1|) | \mu^- \rangle$ is,

$$\frac{1}{2^n \cdot (V_{\max} - V_{\min})} \left((V_{\min} - V_{\min}) + \sum_{S \subseteq F \setminus \{i\}} \gamma(|F \setminus \{i\}|, |S|) \cdot (V^+(S) - V^-(S)) \right). \quad (13)$$

Applying the definition of V^+ and V^- gives the result. ■

The Shapley value $\Phi(i)$ can be obtained by repeatedly creating the quantum systems $|\mu^+\rangle$ and $|\mu^-\rangle$, measuring their last qubit, subtracting their averages, and finally multiplying by $2^n \cdot (V_{\max} - V_{\min})$. However, this representation requires an exponential number of queries to B^\pm to estimate. Additionally, this naive implementation of B^\pm requires an exponential number of terms to be implemented. In the following section, we develop a more efficient solution for the Shapley value calculation of cooperative games.

5 EFFICIENT QUANTUM ALGORITHM FOR SHAPLEY VALUE APPROXIMATION

Consider an $n + 1$ player game G . Suppose we have a quantum representation of the function $\hat{V}^\pm(S)$, defined in Equation (8), which acts on two registers, a player register, and a utility register. Additionally, we introduce a third register, called the partition register, which we use to generate the weights in the Shapley value sum. Table 2 gives an overview of some of the notation in this and the previous section (Sections 4 and 5), while Table 3 provides an overview for the remainder of the section.

Table 3. Notation and symbols used in sections 5 and 7

ϵ	: Total error of the efficient Shapley value approximation algorithm (Section 5)
Partition Register	: Partition register Pt helps to prepare an amplitude distribution that corresponds to the $\gamma(n, m)$'s in the Shapley Equation (1)
U_V^\pm	: U_V^- is a quantum implementation of \hat{V}^- , which outputs to the utility register, Equation (14) : U_V^+ is a quantum implementation of \hat{V}^+ , which outputs to the utility register, Equation (14)
$ V^\pm(h)\rangle$: $ V^-(h)\rangle$ is the result of applying U_V^- to the utility register with input integer h , Equation (15) : $ V^+(h)\rangle$ is the result of applying U_V^+ to the utility register with input integer h , Equation (15)
$b_{n,m}(x)$: Proportional to the Binomial distribution where x is probability of success, n is the number of trials, and m is the number of successes (Definition 6)
$\beta_{n,m}$: Integral of $b_{n,m}(x)$ from 0 to 1 (Definition 6), $\beta_{n,m}$ is precisely equal to $\gamma(n, m)$ (Theorem 3)
P_ℓ	: Partition of the interval from 0 to 1, made up of 2^ℓ points, Equation (17)
$t_\ell(k)$: Location of the k th point in the partition P_ℓ , Equation (18)
$w_\ell(k)$: Width of the k th subinterval of partition P_ℓ , Equation (19)
D_ℓ	: Quantum algorithm which prepares a state with amplitudes $\alpha_k \approx w_\ell(k)$, Equation (20)
H_m	: Set of binary strings h of a fixed length (i.e., n) such that $ h _H = m$ (Lemma 2)
$C_D(\ell)$: Complexity of implementing D_ℓ (Definition 8)
$C_V(\epsilon')$: Complexity of implementing U_V^\pm with maximum error upper bounded by ϵ' (Definition 12)
R_j	: Takes partition register as input and rotates the j th player qubit accordingly, Equation (21)

Approximating the Shapley value with additive error bounded by ϵ with success probability at least $8/\pi^2$ consists of the following steps:

- (1) Represent every possible subset of players in a quantum superposition, excluding player i , with probability amplitudes corresponding to weights $\gamma(n, m)$ in the Shapley Equation (1).
- (2) Perform the quantum version of V^\pm controlled by the player registers, while also potentially using a zeroed auxiliary register, on the utility register. If V^+ (respectively V^-) is applied, then the expected value of measuring the utility register corresponds to $\Phi^+(i)$ (respectively $\Phi^-(i)$).

From this point, it is possible to approximate the Shapley value $\Phi(i)$ if one has the expected value of measuring the utility register.

- (3) To approximate the expected value of measuring the utility register while introducing ϵ' error, perform amplitude estimation with $O((V_{\max} - V_{\min})/\epsilon')$ iterations, where Step 1 is \mathcal{A} and Step 2 is V^\pm as defined in Montanaro [22].

The final error is less than or equal to ϵ with a fixed predetermined probability. Analysis for error propagation of each step is included in Appendix D.

Efficient Quantum Algorithm for Shapley Value Approximation

Input: Game $G = (F, V)$, where F is a set of $n + 1$ players, a quantum implementation U_V^\pm of the value function V^\pm , a player i , and error bound ϵ .

Begin with $|\psi_0\rangle$, a quantum state with three registers, i.e.,

$$|\psi_0\rangle = |0\rangle_{\text{Pt}} \otimes |0\rangle_{\text{P1}} \otimes |0\rangle_{\text{Ut}}.$$

where the partition register Pt has $\ell = O(\log((V_{\max} - V_{\min}) \cdot \sqrt{n}/\epsilon))$ qubits, player register P1 is n qubits, and utility register Ut is one qubit. The partition register helps prepare an amplitude distribution corresponding to the $\gamma(n, m)$'s in the Shapley Equation (1). The player register stores a superposition of all possible player coalitions. A player is excluded or included from a coalition if the bit in the player register with position corresponding to their number, is 0 or 1. The value of each coalition is encoded in the amplitudes of the Utility register qubit.

Step 1: Prepare the partition register such that,

$$|\psi_{1a}\rangle = \sum_{k=0}^{2^\ell-1} \sqrt{w_\ell(k)} |k\rangle_{\text{Pt}} |0\rangle_{\text{P1}} |0\rangle_{\text{Ut}}.$$

where $w_\ell(k) = \sin^2(\pi(k+1)/2^{\ell+1}) - \sin^2(\pi k/2^{\ell+1})$. Then, apply the circuit R_j from Figure 1, described mathematically in Equation (21), to each player qubit, $j \in \{0, 1, \dots, i-1, i+1, \dots, n-1, n\}$. This yields the state $|\psi_{1b}\rangle$ (Equations (22) and (23)) which gives a superposition of all player coalitions with probability amplitudes that correspond to $\gamma(n, m)$ in Equations (2) and (3).

Step 2: Apply the quantum implementation of the value function U_V^+ where player i is included, that uses the player register as an input and outputs to the utility register's amplitudes. This gives $|\psi_2^+\rangle$.

Step 3: Next, use the quantum subroutine to estimate a function's mean with bounded outputs from Montanaro [22]. This approximates the expected value of measuring the utility register for $|\psi_2^+\rangle \approx \Phi^+(i)$.

Repeat Steps 1 to 3 using the quantum implementation of the value function U_V^- where player i is excluded, yielding an approximation for $\Phi^-(i)$. Finally, we approximate the Shapley value of player i , $\Phi(i)$, as the difference $\Phi^+(i) - \Phi^-(i)$.

We now describe the details of the algorithm. The goal is to efficiently approximate the Shapley value $\Phi(i)$ of a given player $i \in F$. We individually find $\Phi^+(i)$ and $\Phi^-(i)$ to simplify the quantum circuits. Suppose the quantum representation of the function $\hat{V}^\pm(h)$, defined in Equation (8), is given as:

$$U_V^\pm |h\rangle_{\text{P1}} |0\rangle_{\text{Ut}} := |h\rangle_{\text{P1}} |V^\pm(h)\rangle_{\text{Ut}} \quad (14)$$

where $|h\rangle$ is a vector in the computational basis (i.e., $h \in \{0, 1\}^n$), and where,

$$|V^\pm(h)\rangle := \sqrt{1 - \hat{V}^\pm(h)} |0\rangle + \sqrt{\hat{V}^\pm(h)} |1\rangle \quad (15)$$

A critical step for the algorithm is to approximate the weights of the Shapley value function. These weights correspond perfectly to a modified beta function.

DEFINITION 6 (MODIFIED BETA FUNCTION). *Let $n \in \mathbb{N}$ and $m \in \{0, \dots, n\}$. We define the beta function as:*

$$\beta_{n,m} = \int_0^1 b_{n,m}(x) dx, \text{ where}$$

$$b_{n,m}(x) = x^m (1-x)^{n-m}.$$

THEOREM 3. *The beta function $\beta_{n,m}$ is equal to the Shapley weight function $\gamma(n, m)$, for $n \in \mathbb{N}$ and $m \in \{0, \dots, n\}$.*

PROOF. See Appendix B. ■

The beta function and, by extension, the Shapley weights are approximated with Riemann sums. The sums represent the area under the function $x^m(1-x)^{n-m}$ using partitions of the interval $[0, 1]$. We demonstrate the function $x^m(1-x)^{n-m}$ can be implemented efficiently on a quantum computer.

DEFINITION 7 (RIEMANN SUM). *A Riemann sum [23, page 276] of a function f , with respect to a partition $P = (t_0, \dots, t_s)$ of the interval $[a, b]$, is an approximation of the integral of f from a to b of the form:*

$$\sum_{k=0}^{s-1} (t_{k+1} - t_k) \cdot f(x_k)$$

where $t_{k+1} - t_k$ is the width of the subinterval, and $f(x_k)$ is the height, $x_k \in [t_k, t_{k+1}]$.

We begin with the initial quantum state:

$$|\psi_0\rangle = |0\rangle_{\text{Pt}}^{\otimes \ell} \otimes |0\rangle_{\text{P1}}^{\otimes n} \otimes |0\rangle_{\text{Ut}}, \quad (16)$$

where Pt, P1, and Ut denote the partition, player, and utility registers. We leverage Pt to prepare the $\gamma(n, m)$ weights. Let $\ell \in \mathbb{N}$ be the number of qubits in Pt, with $\ell = \lceil \log_2((V_{\max} - V_{\min})\sqrt{n}/\epsilon) \rceil + 5$, where ϵ represents the desired error (follows from Theorem 7). Let the number of qubits in the player register be n , one qubit per player excluding player i . Note, in practice, there will often be a qubit to represent player i ; however, we omit this qubit for simplicity. Let the number of qubits in the utility register be one.

Consider the partition,

$$P_\ell = (t_\ell(k))_{k=0}^{2^\ell}, \quad (17)$$

of the interval $[0, 1]$, leveraged for Riemann sums in Figure 2, where,

$$t_\ell(k) := \sin^2\left(\frac{k\pi}{2^{\ell+1}}\right), \text{ with } k = 0, 1, \dots, 2^\ell. \quad (18)$$

This partition is computationally simple to implement on a quantum computer. Let us define $w_\ell(k)$ to be the width of the k th subinterval of P_ℓ , with $k = 0, 1, \dots, 2^\ell - 1$,

$$w_\ell(k) := t_\ell(k+1) - t_\ell(k). \quad (19)$$

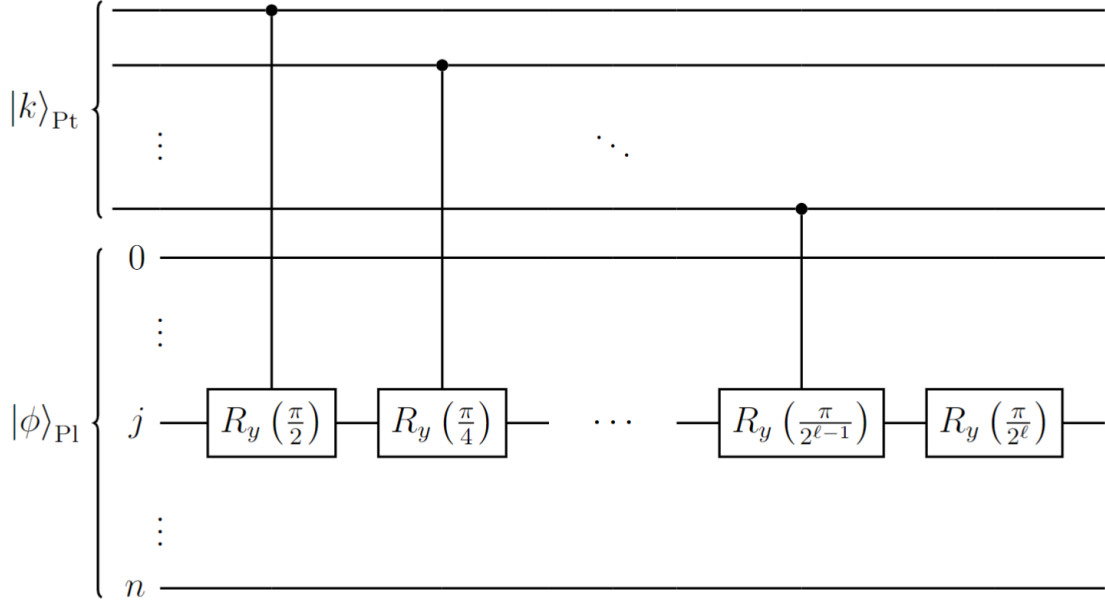


Fig. 1. This circuit R_j is a controlled rotation of the j th player qubit, where $R_y(\theta) = (\cos(\theta/2), -\sin(\theta/2); \sin(\theta/2), \cos(\theta/2))$. (Note: Library used for visualizing circuits can be found here in Ref. [26]).

Let us prepare the partition register to be,

$$D_\ell |0\rangle_{\text{Pt}}^{\otimes \ell} = \sum_{k=0}^{2^\ell-1} \sqrt{w_\ell(k)} |k\rangle_{\text{Pt}}. \quad (20)$$

Note that $\sqrt{w_\ell(k)}$ is real and positive for all k , and that $\sum_{k=0}^{2^\ell-1} w_\ell(k) = 1$. Thus, D_ℓ can be implemented as a unitary. Any approximation of Equation (20), with a maximum error for $w_\ell(k)$ of $\mathcal{O}(4^{-n})$, is compatible with the error analysis in Appendix D.

DEFINITION 8. We denote $C_D(\ell)$ as the complexity to implement D_ℓ such that it satisfies,

$$\max_{k \in \{0,1\}^\ell} |\langle k | D_\ell | 0 \rangle^{\otimes \ell} - w_\ell(k)| \leq \mathcal{O}(4^{-\ell}),$$

Unfortunately, approximating a state to such a high accuracy is currently computationally intensive to implement. It is still an area of active research [24]. At the very least, D_ℓ can be implemented without error in $(23/24)2^\ell$ CNOT gates [25]. For the remainder of this work, we use a placeholder for the complexity $C_D(\ell) \leq (23/24)2^\ell < 32(V_{\max} - V_{\min})\sqrt{n}/\epsilon$.

The new state of the quantum system becomes,

$$\begin{aligned} |\psi_{1a}\rangle &= (D_\ell \otimes I^{\otimes n} \otimes I) |\psi_0\rangle \\ &= \sum_{k=0}^{2^\ell-1} \sqrt{w_\ell(k)} |k\rangle_{\text{Pt}} |0\rangle_{\text{Pl}} |0\rangle_{\text{Ut}}. \end{aligned}$$

Define R_j to be the $(\ell + n)$ -qubit unitary controlled by the partition register acting as a rotation on the j th player qubit and acting as identity on every other player qubit (Figure 1).

$$R_j |k\rangle_{\text{Pt}} |0\rangle_{\text{P1}}^{\otimes n} := |k\rangle_{\text{Pt}} \otimes \left(|0\rangle^{\otimes j} \otimes \left(\sqrt{1 - t'_\ell(k)} |0\rangle + \sqrt{t'_\ell(k)} |1\rangle \right) \otimes |0\rangle^{\otimes n-j-1} \right)_{\text{P1}} \quad (21)$$

where $t'_\ell(k) = t_{\ell+1}(2k + 1)$ is used to sample the height of the k^{th} subinterval in the Riemann sum. Note that the value of $t'_\ell(k)$ is always somewhere in the range $[t_\ell(k), t_\ell(k + 1)]$ (Appendix C).

Unitary R_j is performed on each qubit in the player register, controlled by the partition register. The sum of all applications of R_j can be performed with $n\ell$ gates in $O(\max(n, \ell))$ layers and yields the quantum state:

$$|\psi_{1b}\rangle = \prod_{j=0}^n (R_j \otimes I) |\psi_{1a}\rangle \quad (22)$$

$$= \sum_{k=0}^{2^\ell-1} \sqrt{w_\ell(k)} |k\rangle_{\text{Pt}} \left(\sqrt{1 - t'_\ell(k)} |0\rangle + \sqrt{t'_\ell(k)} |1\rangle \right)_{\text{P1}}^{\otimes n} |0\rangle_{\text{Ut}}. \quad (23)$$

Recall that the player register is of size n qubits. By performing R_j on each qubit, given a particular $|k\rangle_{\text{Pt}}$, each player qubit has been rotated by $t'_\ell(k)$. The reason for doing this is non-trivial and justified in Lemma 2. In short, this operation is equivalent to sampling the heights of the $b_{n,m}$ function in every subinterval of the partition P_ℓ . We use the resulting values in a Riemann sum approximation of the special beta function.

LEMMA 2. *Let H_m be the set of binary numbers of hamming distance m from 0 in n bits, such that $h \in H_m$ implies $|h|_H = m$ (Equation (11)). We have the following relation:*

$$\left(\sqrt{1 - t'_\ell(k)} |0\rangle + \sqrt{t'_\ell(k)} |1\rangle \right)^{\otimes n} = \sum_{m=0}^n \sqrt{b_{n,m}(t'_\ell(k))} \sum_{h \in H_m} |h\rangle.$$

PROOF. We can rewrite our state as,

$$\left(\sqrt{1 - t'_\ell(k)} |0\rangle + \sqrt{t'_\ell(k)} |1\rangle \right)^{\otimes n} = \sum_{h=0}^{2^n-1} \alpha_h |h\rangle.$$

where $\sum_{h=0}^{2^n-1} |\alpha_h|^2 = 1$, $\alpha_h \in \mathbb{C}$. Noting that $\cup_{m=0}^n H_m = \{0, 1, \dots, 2^n - 1\}$, and $j \neq s$ implies $H_j \cap H_s = \emptyset$. We find,

$$\sum_{h=0}^{2^n-1} \alpha_h |h\rangle = \sum_{m=0}^n \sum_{h \in H_m} \alpha_h |h\rangle.$$

Taking $h = h_n \cdots h_{i+1} h_{i-1} \cdots h_0 \in \{0, 1\}^n$, α_h can be defined as follows,

$$\begin{aligned} \alpha_h &= \prod_{j=0}^n \left(-h_j \sqrt{1 - t'_\ell(k)} + h_j \sqrt{t'_\ell(k)} \right) \\ &= \sqrt{t'_\ell(k)^{|h|_H}} \left(1 - t'_\ell(k) \right)^{n-|h|_H} \\ &= \sqrt{b_{n,|h|_H}(t'_\ell(k))}. \end{aligned}$$

where $-0 = 1$ and $-1 = 0$. The last step of the equality chain is based on Definition 6. Since for all $h \in H_m$, $|h|_H = m$, the result holds. ■

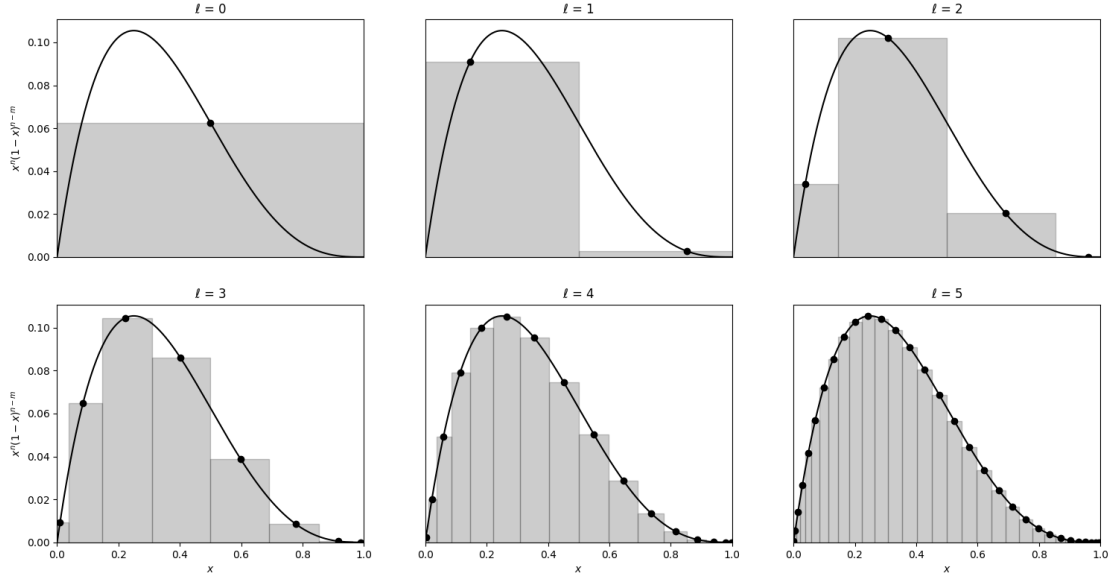


Fig. 2. Visual representation of $\beta_{n,m}$ being approximated using Riemann sums of function $b_{n,m}(x) = x^m(1-x)^{n-m}$ over partition P_t , $t \in [0, 1]$, $n = 4$, $m = 1$. The k^{th} rectangle's height is $b_{n,m}(t'_l(k)) = (t'_l(k))^m(1 - t'_l(k))^{n-m}$, and its width is $w_l(k)$.

Then, by Lemma 2, we can rewrite $|\psi_{1b}\rangle$ as:

$$|\psi_{1b}\rangle = \sum_{k=0}^{2^\ell-1} \sqrt{w_\ell(k)} |k\rangle_{\text{Pt}} \cdot \sum_{m=0}^n \sqrt{b_{n,m}(t'_\ell(k))} \cdot \sum_{h \in H_m} |h\rangle_{\text{P1}} |0\rangle_{\text{Ut}}$$

Note that, with this encoding style for S_h , h 's hamming distance from 0 in h bits equals the size of S_h . In other words, if $h \in H_m$, then S_h contains m players.

Rearranging the quantum state $|\psi_{1b}\rangle$ gives,

$$|\psi_{1b}\rangle = \sum_{m=0}^n \sum_{h \in H_m} \sum_{k=0}^{2^\ell-1} \sqrt{w_\ell(k) b_{n,m}(t'_\ell(k))} |k\rangle_{\text{Pt}} |h\rangle_{\text{P1}} |0\rangle_{\text{Ut}}.$$

Next, we perform V^\pm on the utility register controlled by the player register. Applying $U_V^\pm |h\rangle_{\text{P1}} |0\rangle_{\text{Ut}}$ (Equation (14)) gives $|\psi_2^\pm\rangle$, which is equal to,

$$\begin{aligned} |\psi_2^\pm\rangle &= (I^{\otimes \ell} \otimes U_V^\pm) |\psi_{1b}\rangle \\ &= \sum_{m=0}^n \sum_{h \in H_m} \sum_{k=0}^{2^\ell-1} \sqrt{w_\ell(k) b_{n,m}(t'_\ell(k))} |k\rangle_{\text{Pt}} |h\rangle_{\text{P1}} |V^\pm(h)\rangle_{\text{Ut}}. \end{aligned}$$

This operation is wholly dependent on the complexity of the game being analyzed. Assuming the algorithm is implemented with a look-up table, one could likely use qRAM [27]. This approach has a time complexity of $\mathcal{O}(n)$ at the cost of $\mathcal{O}(2^n)$ qubits for storage. However, depending on the problem, there are often far less resource-intense

methods of implementing U_V^\pm , as is seen with the implementation of weighted voting games (Section 6). In Appendix D, approximate implementations of U_V^\pm and the resulting error propagation are analyzed.

This is the final quantum state. Let us now analyze this state through the lens of density matrices. Taking the partial trace with respect to the partition (Pt) and player (P1) registers yields,

$$\text{tr}_{\text{Pt}, \text{P1}} (|\psi_2^\pm\rangle\langle\psi_2^\pm|) = \sum_{m=0}^n \sum_{h \in H_m} \left(\sum_{k=0}^{2^\ell-1} w_\ell(k) b_{n,m}(t'_\ell(k)) \right) \cdot |V^\pm(h)\rangle_{\text{Ut}} \langle V^\pm(h)|_{\text{Ut}}.$$

THEOREM 4. *The Riemann sum using partition P_ℓ to approximate area under $x^m(1-x)^{n-m}$ for $x \in [0, 1]$ asymptotically approaches $\gamma(n, m)$. Formally,*

$$\sum_{k=0}^{2^\ell-1} w_\ell(k) b_{n,m}(t'_\ell(k)) = \gamma(n, m) + \epsilon' \quad (24)$$

where $|\epsilon'| \leq \pi/2^\ell$.

PROOF. Demonstrated in Appendix D, in particular, see Definition 10, and Lemma 11. ■

The Riemann sum approximation of the modified beta function, $\beta_{n,m} = \gamma(n, m)$ (Theorem 3), is visualized in Figure 2. Applying our approximation for $\gamma(n, m)$ and tracing out the *player* and *partition* registers, we have,

$$\text{tr}_{\text{Pt}, \text{P1}} (|\psi_2^\pm\rangle\langle\psi_2^\pm|) \approx \sum_{m=0}^n \sum_{h \in H_m} \gamma(n, m) |V^\pm(h)\rangle_{\text{Ut}} \langle V^\pm(h)|_{\text{Ut}}.$$

Finally, suppose we measure the utility register on a computational basis. This yields the following expected value with error less than $(V_{\max} - V_{\min})\sqrt{n}/2^{\ell-3}$ (Appendix D),

$$\sum_{m=0}^n \sum_{h \in H_m} \gamma(n, m) \hat{V}^\pm(h).$$

Comparing the expected values of measuring the utility registers for $|\psi_2^+\rangle$ and $|\psi_2^-\rangle$ gives,

$$\sum_{m=0}^n \sum_{h \in H_m} \gamma(n, m) \hat{V}^+(h) - \sum_{m=0}^n \sum_{h \in H_m} \gamma(n, m) \hat{V}^-(h).$$

Plugging in the definition for \hat{V}^\pm , we have,

$$\frac{1}{V_{\max} - V_{\min}} \sum_{m=0}^n \sum_{h \in H_m} \gamma(n, m) (V(S_h \cup \{i\}) - V(S_h)).$$

Notice that in the S_h encoding, H_m represents each subset of $F \setminus \{i\}$ of size m . As a result, the equation is in effect, summing over each subset of $F \setminus \{i\}$ with corresponding γ weights, Definition 3. Thus, multiplying the previous equation by $(V_{\max} - V_{\min})$, we obtain,

$$\sum_{S \subseteq F \setminus \{i\}} \gamma(|F \setminus \{i\}|, |S|) \cdot (V(S \cup \{i\}) - V(S)).$$

This expected value is precisely the Shapley value $\Phi(i)$ to some error analytically upper-bounded in Appendix D. With the ability to craft these states, we can now extract the required information to find a close approximation to the Shapley value. Assuming we could get the expected value instantly, we would have an error of less than $16(V_{\max} - V_{\min})\sqrt{n}/2^\ell$. However, it takes some work to approximate an expected value. This can be achieved with accuracy ϵ with some chosen

confidence using amplitude estimation as described by Montanaro [22], resulting in a circuit which repeats Steps 1 and 2 in the order of $O(\epsilon^{-1})$ times.

To conclude, by Appendix D Theorem 8, we have time complexity in $O(\lambda(C_D(\lceil \log_2(\lambda\sqrt{n}) \rceil) + C_V(\lambda^{-1}) + n \log_2(\lambda\sqrt{n})))$. Where λ is equal to $(V_{\max} - V_{\min})/\epsilon$, ϵ is the desired maximum error with fixed likelihood of success, $C_D(\lceil \log_2(\lambda\sqrt{n}) \rceil)$ is the complexity of implementing $D_{\lceil \log_2(\lambda\sqrt{n}) \rceil}$ with max error $O(\lambda^{-2}n^{-1})$ (Definition 8), and $C_V(\lambda^{-1})$ is the complexity of implementing U_V^\pm with maximum error of λ^{-1} (Appendix D, Definition 12). Assuming a case where $C_V(\lambda^{-1})$ is proportional to or larger than $C_D(\log_2(\lambda\sqrt{n})) + n \log_2(\lambda\sqrt{n})$, the difference $V_{\max} - V_{\min}$ is proportional to σ and $C_V(\epsilon/(V_{\max} - V_{\min}))$ is proportional to $C_V(\epsilon)$, we have a quadratic improvement over Monte-Carlo methods. In the following section, we demonstrate concrete examples of the algorithm.

6 QUANTUM SHAPLEY VALUE EXAMPLES

6.1 Weighted Voting Games

Perhaps we can help David solve his problem (cf. Subsection 3.1) using our quantum approach. We intend to apply the method presented in Section 5 for weighted voting games. Additional results, together with the simulation code, are available in a companion GitHub repository [28]. Let us approximate each player's Shapley value, $\Phi(i)$. We have a game $G = (F, V)$, where $F = \{0, 1, 2\}$, $n = 2$, and V is defined in Equation (4). Let the voting weights be $w_0 = 3$, $w_1 = 2$, and $w_2 = 1$. Thus, we can define $V^\pm(h)$, $h \in \{0, 1\}^2$, where h represents an element in $\mathcal{P}(F \setminus \{i\})$,

$$V^-(h) = \begin{cases} 1 & \text{if } \sum_{s \in S_h} w_s \geq q \\ 0 & \text{otherwise} \end{cases} \quad V^+(h) = \begin{cases} 1 & \text{if } \sum_{s \in S_h \cup \{i\}} w_s \geq q \\ 0 & \text{otherwise} \end{cases}$$

Note that, $V^\pm(h)$ is either 0 or 1. Thus, we can take $V_{\max} = 1$, $V_{\min} = 0$. We define U_V^\pm to be:

$$U_V^\pm |x\rangle |0\rangle = |x\rangle \otimes \left[(1 - \hat{V}^\pm(x)) |0\rangle + \hat{V}^\pm(x) |1\rangle \right]$$

The quantum circuit for the scenario is shown in Figure 3. Note that, much like with the figure, it is trivial to generate V^+ and V^- if one has a quantum gate to compute V .

With U_V^\pm defined, all other steps are entirely agnostic to voting games. Let ℓ be equal to 2, and suppose we can instantly extract the expected value for simplicity's sake. This is not a realistic scenario, but it demonstrates how quickly the expected value of the utility register converges in Steps 1 and 2. With these parameters, we get the following approximations for the Shapley values:

$$\tilde{\Phi}_0 \approx 0.6617, \quad \tilde{\Phi}_1, \tilde{\Phi}_2 \approx 0.1616$$

The direct calculation for Alice can be seen in Appendix A.

To rigorously demonstrate efficacy, we performed many trials on random weighted voting games (Figure 4). Visual inspection confirms that the error from Step 1 decreases exponentially with respect to ℓ . Step 2 depends entirely on the game. However, if it is possible to implement on a classical computer, much like with Grover's algorithm, it can be implemented in a quantum setting [29]. Step 3 is well studied, it extracts the expected value of measuring the utility register with error ϵ , with a fixed probability of success. Use amplitude estimation as described in Section 5 with the techniques described in [22].

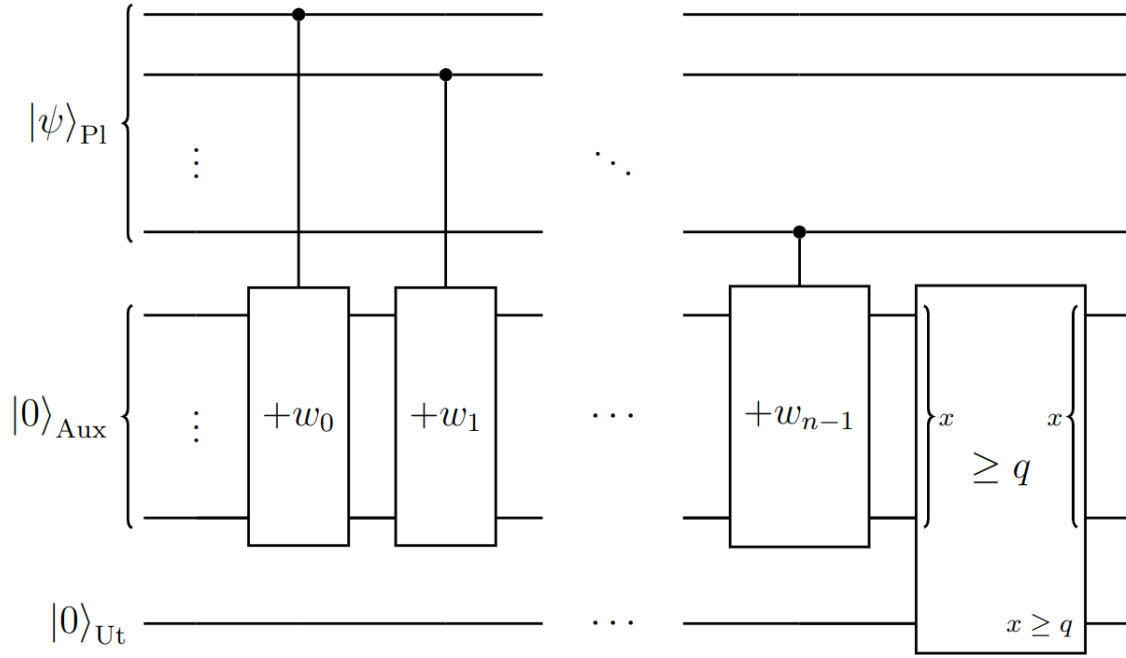


Fig. 3. Circuit of U_V^\pm for a weighted voting game. This circuit takes an basis state input $|h_n, \dots, h_{i+1}, x, h_{i-1}, \dots, h_0\rangle$ and outputs $|V^-(S_h)\rangle$ when $x = 0$ or $|V^+(S_h)\rangle$ when $x = 1$ to the utility register (Recall, S_h is defined in Definition 5). The auxiliary register contains the total vote count. Just before the $\geq q$ gate, the *Aux* register is in a basis state corresponding to the vote count of S_h , including or excluding player i 's vote depending on x . The $\geq q$ gate uses the auxiliary register as an input and outputs whether the vote count exceeds threshold q in the *Ut* register. After this gate, it is trivial to clear the *Aux* register by subtracting each player's contribution. Results and simulation code are available in a companion GitHub repository [28].

6.2 Explainability and Shapley Values of Quantum Binary Classifiers

The local explanation method described in Subsection 3.2 is conveniently translated to the quantum context. Suppose we are given a quantum classifier U_C that acts on two registers as follows, $U_C |j\rangle_{P1} |0\rangle_{Ut} \rightarrow |j\rangle_{P1} |C(j)\rangle$, where $j \in \{0, 1\}^{r \times r}$, and C is defined in Subsection 3.2. To calculate the i th player's Shapley value Φ_i of $V_{C,x}$, Equation (5), and hence generate a local explanation for the model decision $C(x) = y$, we only need a simple modification to our method. We now give a sketch of the implementation. Suppose that, after Step 1 of the Section 5 algorithm, we have the approximate state,

$$\text{tr}_{Pt} |\psi_{1b}\rangle\langle\psi_{1b}| \approx \sum_{m=0}^n \sum_{h \in H_m} \gamma(n, m) |h\rangle_{P1} \langle h|_{P1},$$

ignoring the *Ut* register. To craft the distribution which gives value function $V_{x,C}$, Equation (5), we add a second player register $|0\rangle_{P1'}^{\otimes n}$. We can then apply NOT gates to each qubit in *P1*'. Next, apply controlled Hadamard gates between the previous and new player registers. In particular for each player j , the j th qubit in the *P1*' register controls a Hadamard transform on the j th qubit of the *P1*' register. We proceed with old player register *P1*' traced out. In the remaining Steps, we treat *P1*' as the player register. If we continue with the other steps of the algorithm, Steps 2 and 3, the output will be the Shapley value Φ_i of corresponding to $V_{C,x}$.

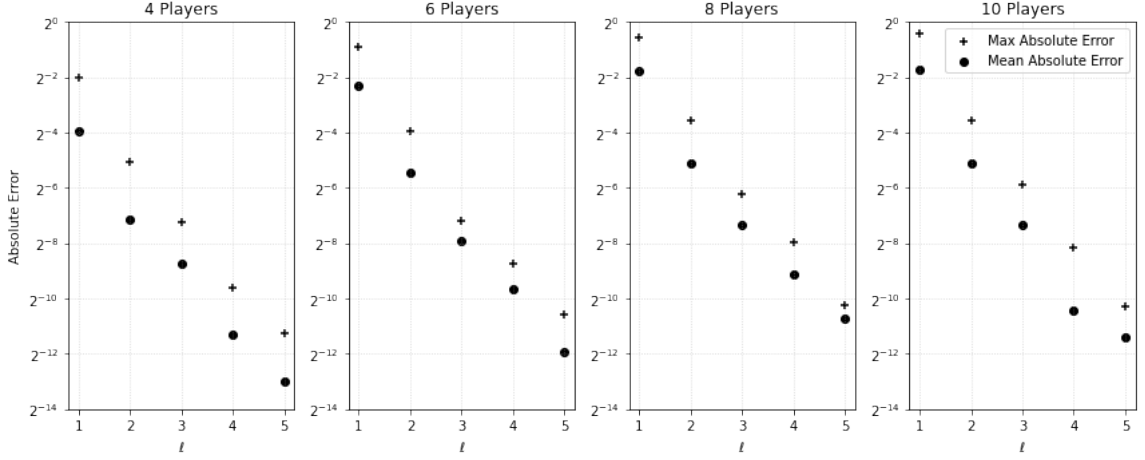


Fig. 4. This figure demonstrates the exponentially small error introduced in Step 1 with respect to ℓ . We generated 64 random weighted voting games for each condition, e.g., for each combination of ℓ and number of players. Random weights $w_j \in \mathbb{N}$ were assigned for each case such that $q \leq \sum_j w_j < 2q$. There were four primary scenarios: (1) Four players, voting threshold $q = 8$; (2) Six players, voting threshold $q = 16$; (3) Eight players, voting threshold $q = 32$; and (4) Ten players, voting threshold $q = 32$. We approximated every player's Shapley value for each scenario with our quantum algorithm using various ℓ 's, taking only Step 1's error into account. Next, we found the absolute error of our approximation by comparing each approximated Shapley value to its true value. The graphs show the mean and maximum absolute errors of each condition. Results and simulation code are available in a companion GitHub repository [28].

7 IMPROVED QUANTUM ALGORITHM FOR SHAPLEY VALUE APPROXIMATION

Section 5 describes an algorithm to estimate the Shapley values of cooperative games. Assuming a reasonable implementation of D_ℓ (20), the algorithm is often more efficient than classical random sampling. However, an implementation of D_ℓ may not be realistic in the short term, as it might require repeatedly calculating the square root of \sin [24]. Additionally, current techniques may not converge quickly enough to D_ℓ to give an advantage over classical methods. As a result, we want to avoid the use of D_ℓ .

Previously, the matrix D_ℓ was used to compensate for the peculiar partition P_ℓ (17), a consequence of using the circuit from Figure 1. If we can create a more reasonable partition, we will not need such expensive compensations. In particular, we can leverage the Quantum CORDIC algorithm for approximation of \arcsin to sample from $b_{n,m}(x)$ uniformly [30]. This can be combined with the uniform partition,

$$Q_\ell = \left(k2^{-\ell} \right)_{k=0}^{2^\ell}, \quad (25)$$

to approximate the γ Shapley weights, Definition 3. The partition Q_ℓ has the desirable property that each subinterval has a width equal to $2^{-\ell}$, which is easily implemented with Hadamard gates.

Consider the $n + 1$ player game as defined in Section 5, we wish to find the Shapley value Φ_i of the i th player. By [30], leveraging $4\ell + O(\log \ell)$ zeroed auxiliary qubits, and using $O(\ell^2)$ CNOTs, we can perform the following operation,

$$\frac{1}{\sqrt{2^\ell}} \sum_{k=0}^{2^\ell-1} |k\rangle_{\text{Pt}} |0\rangle \rightarrow \frac{1}{\sqrt{2^\ell}} \sum_{k=0}^{2^\ell-1} |k\rangle_{\text{Pt}} \left(\sqrt{1-r_\ell(k)} |0\rangle + \sqrt{r_\ell(k)} |1\rangle \right),$$

where $r_\ell(k) = (k + 1/2)2^{-\ell} + \epsilon_k$, and $|\epsilon_k|$ is less than $2^{-(\ell+1)}$. It follows that $r_\ell(k) \in [k2^{-\ell}, (k+1)2^{-\ell}]$. This can be applied to each player qubit, yielding state,

$$\frac{1}{\sqrt{2^\ell}} \sum_{k=0}^{2^\ell-1} |k\rangle_{\text{Pt}} \left(\sqrt{1-r_\ell(k)} |0\rangle + \sqrt{r_\ell(k)} |1\rangle \right)_{\text{P1}}^{\otimes n}.$$

Using a nearly identical argument to Lemma 2, and some rearrangement, this is equal to,

$$\sum_{m=0}^n \sum_{H_m} \sum_{k=0}^{2^\ell-1} \sqrt{\frac{b_{n,m}(r_\ell(k))}{2^\ell}} |k\rangle_{\text{Pt}} |h\rangle_{\text{P1}},$$

where $b_{n,m}$ is defined in Definition 6, and H_m is defined in the statement of Lemma 2. We next add the Ut register and perform U_V^\pm , Equation (14), giving state,

$$|\phi^\pm\rangle = \sum_{m=0}^n \sum_{H_m} \sum_{k=0}^{2^\ell-1} \sqrt{\frac{b_{n,m}(r_\ell(k))}{2^\ell}} |k\rangle_{\text{Pt}} |h\rangle_{\text{P1}} |V^\pm(h)\rangle_{\text{Ut}}.$$

Similarly to Section 5, this yields the following expected value for measuring the utility register,

$$\sum_{m=0}^n \sum_{h \in H_m} \left(\sum_{k=0}^{2^\ell-1} \frac{b_{n,m}(r_\ell(k))}{2^\ell} \right) \hat{V}^\pm(h).$$

Notice that $\sum_{k=0}^{2^\ell-1} 2^{-\ell} b_{n,m}(r_\ell(k))$ is a Riemann sum (Definition 7) approximation of $\beta_{n,m}$ (Definition 6), which is equal to $\gamma(n, m)$ (Theorem 3). Combining the reasoning of Corollary 3 and Lemma 11, our Riemann sum approximates $\gamma(n, m)$ with absolute error less than $2^{1-\ell} b_{n,m}(m/n)$. As a result, our final error using this method will be less than the bound for the previous algorithm described in Section 5, thus, the error analysis of Appendix D still applies for any given ℓ .

THEOREM 5. *The expected value of the Ut register of $|\phi^\pm\rangle$, multiplying by $V_{\max} - V_{\min}$, and subtracting by V_{\min} yields,*

$$\Phi_i + \rho, \quad \rho \in [-\epsilon, \epsilon], \quad \epsilon > 0.$$

Given a fixed probability of success, the operation takes,

$$O\left(\left\lceil \frac{\sqrt{\Delta V(\Phi_i - V_{\min})}}{\epsilon} \right\rceil \cdot \left\lceil \log^2\left(\frac{\Delta V n}{\epsilon}\right) + n \log\left(\frac{\Delta V n}{\epsilon}\right) + C_V\left(\frac{\epsilon}{4\Delta V}\right) \right\rceil\right),$$

operations. Wherein, $\Delta V = V_{\max} - V_{\min}$, and $C_V(x)$ is the complexity of implementing U_V^\pm with maximum error bound x (Definition 12).

PROOF. Follows from Theorem 8 and the replacement of transformation D_ℓ with the transformation described in [30]. In particular, we must perform $O\left(\epsilon^{-1} \sqrt{\Delta V(\Phi_i - V_{\min})}\right)$ iterations of amplitude estimation as described by Montanaro [22]. To prepare the γ distribution, each iteration requires that we apply \arcsin as described in [30], requiring $O(\log^2(\Delta V n / \epsilon))$ steps. The results are encoded in player amplitudes using $O(n \log(\Delta V n / \epsilon))$ operations. Finally, each iteration requires a query to the value function U_V^\pm with maximum error $\epsilon / (4\Delta V)$, taking $O(C_V(\epsilon / (4\Delta V)))$ operations (Definition 12). ■

When the range is not exponentially large, and U_V is even somewhat complex with respect to number of players and error, the γ preparation steps can be ignored in the complexity analysis.

Table 4. Complexity Comparison

Quantum Algorithm	:	$O\left(\frac{\sqrt{(V_{\max}-V_{\min})(\Phi_i-V_{\min})}}{\epsilon} C_V\left(\frac{\epsilon}{4(V_{\max}-V_{\min})}\right)\right)$
Monte-Carlo	:	$O\left(\frac{\sigma^2}{\epsilon^2} C_V(\epsilon)\right)$

COROLLARY 1. Suppose $C_V(\epsilon/(4\Delta V))$ is greater or equal to $O(\log^2(\Delta V n/\epsilon) + n \log(\Delta V n/\epsilon))$, $\Delta V = V_{\max} - V_{\min}$. The expected value of the Ut register of $|\phi^\pm\rangle$, multiplying by $V_{\max} - V_{\min}$, and subtracting by V_{\min} yields,

$$\Phi_i + \rho, \quad \rho \in [-\epsilon, \epsilon], \quad \epsilon > 0.$$

Given a fixed probability of success, the operation takes,

$$O\left(\frac{\sqrt{\Delta V(\Phi_i - V_{\min})}}{\epsilon} C_V\left(\frac{\epsilon}{4\Delta V}\right)\right),$$

operations. $C_V(x)$ is defined in Definition 12. This is compared with Monte Carlo methods in Table 4.

EXAMPLE 1. Let us give a more concrete example, suppose we have a game $G = (F, V)$, where F is an $n + 1$ player game and we have a value function $V : \mathcal{P}(F) \rightarrow \{0, 1\}$. Then V_{\min}, V_{\max} are 0 and 1 respectively. Suppose that U_V^\pm is, as a result, implemented with no error. In this case, the complexity $C_V = C_V(0)$ is fixed (Definition 12), and we assume that C_V is proportional to the complexity of implementing V classically. Suppose we wish to find the i th player's Shapley value Φ_i . We proceed assuming Φ_i is on the interval $[-1/2, 1/2]$. Thus, using classical Monte Carlo methods, V yields a Bernoulli distribution with a variance of $\sigma^2 = \Phi_i(1 - \Phi_i)$, since $|\Phi_i| \leq 0.5$, it follows that $\sigma^2 \in O(\Phi_i)$. We therefore have classical complexity,

$$O\left(\frac{\Phi_i}{\epsilon^2} C_V\right).$$

On the other hand, in the quantum context, we have,

$$O\left(\frac{\sqrt{\Phi_i}}{\epsilon} \left(C_V + \log^2\left(\frac{1}{\epsilon}\right)\right)\right).$$

This follows directly from Theorem 5. Note that n is fixed in this context. This is a quadratic improvement up to polylogarithmic factors.

8 RELATED WORK

Explainability in AI is a quickly growing area of importance, especially given the rise in legislative interest and regulation for transparency in the United States and European Union respectively [1–3]. The post-hoc method of additive explanations in model agnostic contexts is addressed in Riberio et al.'s seminal work [31]. Riberio et al. introduced the model agnostic Local Interpretable Model-agnostic Explanations (LIME) algorithm to assess the importance of each feature for particular decisions. It leveraged the fact that many classifiers, represent differential functions, and are hence locally linear. In addition to Riberio et al.'s work, various additive explanation methods have been introduced, such as layer-wise relevance propagation [32]. Lundberg and Lee [6] found that many of the newly introduced additive explanation methods were equivalent to finding the Shapley values of the input variables. Specifically, each explanation which satisfies a small set of properties is equivalent to a Shapley value approximation. The work culminated in Lundberg and Lee's widely used SHapley Additive exPlanation (SHAP) algorithm. More recently, the particular implementation

of SHAP has come under scrutiny. According to Marques-Silva and Huang [33], there are no rigorous error guarantees for the most popular approximations of SHAP. More concerning, Marques-Silva and Huang claim SHAP’s definition is not formally justified and demonstrates specific circumstances where exact SHAP produces undesirable results. Their criticisms do not necessarily translate to Shapley values but illustrate the need for deep care and caution for robust explainability.

In tandem with additive explanations, there are multiple approaches which aim to make AI more trustworthy. In the domain of post-hoc explanations, there is also the option of counterfactual explanations [19]. A counterfactual expresses how an outcome would be different given different initial conditions. A counterfactual explanation describes what minimal changes could be made to get a more desirable outcome, for example, “*your bank loan would have been accepted if your income had been 10% higher*”. On the other hand, some authors argue that, in high-stakes situations, black box models should be abandoned altogether in favour of inherently interpretable models [4, 34]. These models include purely linear models, decision trees and more. While some believe black-box models have a performance advantage in many domains, Rudin [4] claims that interpretable models have similar potential in many relevant circumstances. Rudin argues that interpretable models allow for better iterative improvements, as their flaws are understandable and therefore easier to address. Additionally, when the data is structured, and effectively preprocessed, Rudin asserts that simple classifiers perform similarly to complex classifiers. However, London [35] argues that in cases where black-box models have higher accuracy, they should not be automatically discarded.

Beyond explainable AI, Shapley values have been widely used to address multiple engineering problems, including regression, statistical analysis, and Machine Learning (ML) [36]. Finding Shapley values presents a difficult computational combinatorial problem. The deterministic computation of Shapley values in weighted voting games is at least as difficult as NP-Hard [7, 8]. Since voting games are some of the simplest cooperative games, this result does not bode well for more complex scenarios. In the context of Shapley values for machine learning, it has also been shown that the calculation of Shapley values is not tractable for regression models [37]. Similarly, on the empirical distribution, finding a Shapley value takes exponential time [38]. While the general case direct Shapley value calculation is extremely computationally complex, this is not the case if we weaken our requirements. Calculating the Shapley for specific games allows for optimizations which leverage the structure of the problem. This has been done, for instance, in the context of games on graphs [39]. The other approach, which is relevant to our work, is based on probabilistic approximations. Specifically, Castro et al. [9] describes a method based on Monte Carlo methods to approximate Shapley values in polynomial time. By Chebyshev’s inequality, Monte Carlo methods have a query complexity of $O(\sigma^2/\epsilon^2)$, which is tenable when compared to naive and exponentially complex methods [22].

Simultaneously, there has been a strong research effort into quantum AI. Quantum principal component analysis is an early example of an efficient quantum algorithm in the domain of AI [40]. This work lead Rebertrost et al.’s [41] algorithm for quantum support vector machines, which Rebertrost et al. claim is exponentially faster than known classical methods in some cases. It has been shown that training quantum neural networks is possible and that they are universal function approximations [42]. In response to the progress in quantum AI, there has been steady growth in the topic of Quantum Explainable AI. Treating the quantum algorithm as a black box allows for the use of LIME [13, 43]. In a similar vein, SHAP and Shapley values have both been leveraged to explain the behaviour of quantum circuits [11, 44], though these works do not leverage quantum effects to accelerate the computation.

9 CONCLUSION

We have introduced a quantum algorithm which allows for a more efficient approximation of Shapley values. The algorithm is often quadratically faster than is possible with classical Monte Carlo methods, up to polylogarithmic factors. In other words, doubling work yields double the precision. In contrast to the quadrupling of work required classically. The algorithm has two potential applications. First, it can be applied directly to accelerate the calculation of Shapley values in cooperative games. Second, we can leverage the algorithm to construct additive explanations of quantum circuits.

For future work, examining practical examples of the quantum algorithm for Shapley values is a source of various interesting problems. This is especially true in cases where the value function can be more efficiently computed on a quantum computer. In a similar vein, specific games can be analyzed so that their structure might be leveraged for larger quantum advantages. For quantum explainability, there are several useful directions to explore. An additional area of inquiry is whether certain models, such as quantum support vector machines, can have their Shapley values computed more efficiently. Finally, our algorithm can be used to better understand proposed quantum AIs.

REFERENCES

- [1] B. Goodman and S. Flaxman. European Union regulations on algorithmic decision-making and a “right to explanation”. *AI magazine*, 38(3):50–57, 2017.
- [2] M. Nisevic, A. Cuypers, and J. De Bruyne. Explainable ai: Can the ai act and the gdpr go out for a date? In *2024 International Joint Conference on Neural Networks (IJCNN)*, pages 1–8. IEEE, 2024.
- [3] L. Nannini, A. Balayn, and A. L. Smith. Explainability in ai policies: A critical review of communications, reports, regulations, and standards in the eu, us, and uk. In *Proceedings of the 2023 ACM conference on fairness, accountability, and transparency*, pages 1198–1212, 2023.
- [4] C. Rudin. Stop explaining black box machine learning models for high stakes decisions and use interpretable models instead. *Nature Machine Intelligence*, 1(5):206–215, 2019.
- [5] I. Burge, M. Barbeau, and J. Garcia-Alfaro. Quantum algorithms for shapley value calculation. In *2023 IEEE International Conference on Quantum Computing and Engineering (QCE)*, volume 1, pages 1–9. IEEE, 2023.
- [6] S. M. Lundberg and S.-I. Lee. A unified approach to interpreting model predictions. *Advances in neural information processing systems*, 30, 2017.
- [7] Y. Matsui and T. Matsui. NP-completeness for calculating power indices of weighted majority games. *Theoretical Computer Science*, 263(1-2):305–310, 2001.
- [8] K. Prasad and J. S. Kelly. NP-completeness of some problems concerning voting games. *International Journal of Game Theory*, 19(1):1–9, 1990.
- [9] J. Castro, D. Gómez, and J. Tejada. Polynomial calculation of the Shapley value based on sampling. *Computers & Operations Research*, 36(5):1726–1730, 2009.
- [10] J. Biamonte, P. Wittek, N. Pancotti, P. Rebentrost, N. Wiebe, and S. Lloyd. Quantum machine learning. *Nature*, 549(7671):195–202, 2017.
- [11] R. Heese, T. Gerlach, S. Mücke, S. Müller, M. Jakobs, and N. Piatkowski. Explaining quantum circuits with shapley values: Towards explainable quantum machine learning. arXiv: 2301.09138, <https://doi.org/10.48550/arXiv.2301.09138>, March 2023.
- [12] I. Burge, M. Barbeau, and J. Garcia-Alfaro. A Quantum Algorithm for Shapley Value Estimation, arXiv:2301.04727, <https://doi.org/10.48550/arXiv.2301.04727>, March 2023.
- [13] S. Deshmukh, B. K. Behera, P. Mulay, E. A. Ahmed, S. Al-Kuwari, P. Tiwari, and A. Farouk. Explainable quantum clustering method to model medical data. *Knowledge-Based Systems*, 267:110413, 2023.
- [14] J. G. Saw, M. C. Yang, and T. C. Mo. Chebyshev inequality with estimated mean and variance. *The American Statistician*, 38(2):130–132, 1984.
- [15] R. J. Aumann. Some non-superadditive games, and their Shapley values, in the Talmud. *International Journal of Game Theory*, 39:1–10, 2010.
- [16] E. Winter. The Shapley value. *Handbook of game theory with economic applications*, 3:2025–2054, 2002.
- [17] S. Hart. Shapley value. In *Game theory*, pages 210–216. The New Palgrave. Palgrave Macmillan, London, 1989.
- [18] L. S. Shapley. *A Value for N-Person Games*. RAND Corporation, Santa Monica, CA, 1952.
- [19] R. M. Byrne. Counterfactuals in Explainable Artificial Intelligence (XAI): Evidence from Human Reasoning. In *IJCAI*, pages 6276–6282, 2019.
- [20] R. Guidotti. Counterfactual explanations and how to find them: literature review and benchmarking. *Data Mining and Knowledge Discovery*, 38(5):2770–2824, 2024.
- [21] G. Chen, Q. Chen, S. Long, W. Zhu, Z. Yuan, and Y. Wu. Quantum convolutional neural network for image classification. *Pattern Analysis and Applications*, 26(2):655–667, 2023.
- [22] A. Montanaro. Quantum speedup of Monte Carlo methods. *Proceedings of the Royal Society A: Mathematical, Physical and Engineering Sciences*, 471(2181):20150301, 2015.

- [23] K. A. Ross. *Elementary analysis*. Springer, New York, NY, 2013.
- [24] A. G. Rattew and B. Koczor. Preparing arbitrary continuous functions in quantum registers with logarithmic complexity. *arXiv preprint arXiv:2205.00519*, 2022.
- [25] M. Plesch and Č. Brukner. Quantum-state preparation with universal gate decompositions. *Physical Review A*, 83(3):032302, 2011.
- [26] A. Kay. Tutorial on the Quantikz package, arXiv: 1809.03842, <https://arxiv.org/abs/1809.03842>, March 2023.
- [27] V. Giovannetti, S. Lloyd, and L. Maccone. Quantum random access memory. *Physical review letters*, 100(16):160501, 2008.
- [28] I. Burge, M. Barbeau, and J. Garcia-Alfaro. Quantum Algorithms for Shapley Value Calculation [extended simulation github repository], github, <https://github.com/iain-burge/QuantumShapleyValueAlgorithm>, May 2023.
- [29] L. K. Grover. A fast quantum mechanical algorithm for database search. In *Proceedings of the twenty-eighth annual ACM symposium on Theory of computing*, pages 212–219, 1996.
- [30] I. Burge, M. Barbeau, and J. Garcia-Alfaro. Quantum cordic–arcsin on a budget. *arXiv preprint arXiv:2411.14434*, 2024.
- [31] M. T. Ribeiro, S. Singh, and C. Guestrin. " why should i trust you?" explaining the predictions of any classifier. In *Proceedings of the 22nd ACM SIGKDD international conference on knowledge discovery and data mining*, pages 1135–1144, 2016.
- [32] S. Bach, A. Binder, G. Montavon, F. Klauschen, K.-R. Müller, and W. Samek. On pixel-wise explanations for non-linear classifier decisions by layer-wise relevance propagation. *PLoS one*, 10(7):e0130140, 2015.
- [33] J. Marques-Silva and X. Huang. Explainability is not a game. *Communications of the ACM*, 67(7):66–75, 2024.
- [34] M. Ghassemi, L. Oakden-Rayner, and A. L. Beam. The false hope of current approaches to explainable artificial intelligence in health care. *The Lancet Digital Health*, 3(11):e745–e750, 2021.
- [35] A. J. London. Artificial intelligence and black-box medical decisions: accuracy versus explainability. *Hastings Center Report*, 49(1):15–21, 2019.
- [36] S. Lipovetsky. Quantum-like data modeling in applied sciences. *Stats*, 6(1):345–353, 2023.
- [37] G. Van den Broeck, A. Lykov, M. Schleich, and D. Suciu. On the tractability of SHAP explanations. *Journal of Artificial Intelligence Research*, 74:851–886, 2022.
- [38] L. Bertossi, J. Li, M. Schleich, D. Suciu, and Z. Vagena. Causality-based explanation of classification outcomes. In *Proceedings of the Fourth International Workshop on Data Management for End-to-End Machine Learning*, pages 1–10, 2020.
- [39] M. K. Tarkowski, T. P. Michalak, T. Rahwan, and M. Wooldridge. Game-theoretic network centrality: A review. *arXiv preprint arXiv:1801.00218*, 2017.
- [40] S. Lloyd, M. Mohseni, and P. Rebentrost. Quantum principal component analysis. *Nature physics*, 10(9):631–633, 2014.
- [41] P. Rebentrost, M. Mohseni, and S. Lloyd. Quantum support vector machine for big data classification. *Physical review letters*, 113(13):130503, 2014.
- [42] K. Beer, D. Bondarenko, T. Farrelly, T. J. Osborne, R. Salzmann, D. Scheiermann, and R. Wolf. Training deep quantum neural networks. *Nature communications*, 11(1):808, 2020.
- [43] L. Pira and C. Ferrie. On the interpretability of quantum neural networks. *Quantum Machine Intelligence*, 6(2):52, 2024.
- [44] P. Steinmüller, T. Schulz, F. Graf, and D. Herr. eXplainable AI for Quantum Machine Learning. *arXiv preprint arXiv:2211.01441*, 2022.
- [45] H. Robbins. A remark on stirling’s formula. *The American mathematical monthly*, 62(1):26–29, 1955.

A Calculation for Alice

Quantum estimation of Alice’s Shapley value by hand. Let ℓ be equal to 2. Note that an auxiliary register stores the vote count. To perform U_V^- , we begin with the state:

$$|00\rangle_{Pt} |000\rangle_{P1} |000\rangle_{Aux} |0\rangle_{Ut}$$

The first qubit of the player register represents Alice, the second represents Bob, and the third represents Charlie.

We perform the first step of the algorithm described in Section 5, yielding:

$$\begin{aligned} & \sum_{k=0}^3 \sqrt{w_2(k)} |k\rangle_{Pt} \left[(1 - t'_2(k)) |000\rangle_{P1} + \sqrt{t'_2(k)(1 - t'_2(k))} |001\rangle_{P1} \right. \\ & \quad \left. + \sqrt{t'_2(k)(1 - t'_2(k))} |010\rangle_{P1} + t'_2(k) |011\rangle_{P1} \right] |000\rangle_{Aux} |0\rangle_{Ut} \end{aligned}$$

Next, we tally the votes. This step is the first half of the circuit in Figure 3, up to but not including the $\geq q$ gate. We get,

$$\sum_{k=0}^3 \sqrt{w_2(k)} |k\rangle_{\text{Pt}} \left[(1 - t'_2(k)) |000\rangle_{\text{P1}} |000\rangle_{\text{Aux}} + \sqrt{t'_2(k)(1 - t'_2(k))} |001\rangle_{\text{P1}} |001\rangle_{\text{Aux}} \right. \\ \left. + \sqrt{t'_2(k)(1 - t'_2(k))} |010\rangle_{\text{P1}} |010\rangle_{\text{Aux}} + t'_2(k) |011\rangle_{\text{P1}} |011\rangle_{\text{Aux}} \right] |0\rangle_{\text{Ut}}.$$

Performing the remainder of U_V^- gives,

$$\sum_{k=0}^3 \sqrt{w_2(k)} |k\rangle_{\text{Pt}} \left[(1 - t'_2(k)) |000\rangle_{\text{P1}} |000\rangle_{\text{Aux}} |0\rangle_{\text{Ut}} + \sqrt{t'_2(k)(1 - t'_2(k))} |001\rangle_{\text{P1}} |001\rangle_{\text{Aux}} |0\rangle_{\text{Ut}} \right. \\ \left. + \sqrt{t'_2(k)(1 - t'_2(k))} |010\rangle_{\text{P1}} |010\rangle_{\text{Aux}} |0\rangle_{\text{Ut}} + t'_2(k) |011\rangle_{\text{P1}} |011\rangle_{\text{Aux}} |0\rangle_{\text{Ut}} \right].$$

Thus, the expected value when measuring the utility register, after performing U_V^- , is $\Phi_2^-(0) = 0$, where $\Phi_\ell^\pm(i)$ is the ℓ th approximation of the i th player's Shapley value.

To perform U_V^+ , the exact same steps are performed except that we flip Alice to the on state,

$$|00\rangle_{\text{Pt}} |100\rangle_{\text{P1}} |000\rangle_{\text{Aux}} |0\rangle_{\text{Ut}}.$$

where the first qubit of the player register represents Alice, the second represents Bob, and the third represents Charlie.

We perform the first step of the algorithm from Section 5, yielding:

$$\sum_{k=0}^3 \sqrt{w_2(k)} |k\rangle_{\text{Pt}} \left[(1 - t'_2(k)) |100\rangle_{\text{P1}} + \sqrt{t'_2(k)(1 - t'_2(k))} |101\rangle_{\text{P1}} \right. \\ \left. + \sqrt{t'_2(k)(1 - t'_2(k))} |110\rangle_{\text{P1}} + t'_2(k) |111\rangle_{\text{P1}} \right] |000\rangle_{\text{Aux}} |0\rangle_{\text{Ut}}$$

Next, we tally the votes. This step is the first half of the circuit in Figure 3, up to but not including the " $\geq q$ " gate. We get,

$$\sum_{k=0}^3 \sqrt{w_2(k)} |k\rangle_{\text{Pt}} \left[(1 - t'_2(k)) |100\rangle_{\text{P1}} |011\rangle_{\text{Aux}} + \sqrt{t'_2(k)(1 - t'_2(k))} |101\rangle_{\text{P1}} |100\rangle_{\text{Aux}} \right. \\ \left. + \sqrt{t'_2(k)(1 - t'_2(k))} |110\rangle_{\text{P1}} |101\rangle_{\text{Aux}} + t'_2(k) |111\rangle_{\text{P1}} |110\rangle_{\text{Aux}} \right] |0\rangle_{\text{Ut}}.$$

Performing the remainder of U_V^+ gives,

$$\sum_{k=0}^3 \sqrt{w_2(k)} |k\rangle_{\text{Pt}} \left[(1 - t'_2(k)) |100\rangle_{\text{P1}} |011\rangle_{\text{Aux}} |0\rangle_{\text{Ut}} + \sqrt{t'_2(k)(1 - t'_2(k))} |101\rangle_{\text{P1}} |100\rangle_{\text{Aux}} |1\rangle_{\text{Ut}} \right. \\ \left. + \sqrt{t'_2(k)(1 - t'_2(k))} |110\rangle_{\text{P1}} |101\rangle_{\text{Aux}} |1\rangle_{\text{Ut}} + t'_2(k) |111\rangle_{\text{P1}} |110\rangle_{\text{Aux}} |1\rangle_{\text{Ut}} \right].$$

Thus, the expected value when measuring the utility register, after performing U_V^+ , is $\Phi_2^+(0) \approx 0.6617$. Hence, the difference between the expected values $\Phi_2(0) = \Phi_2^+(0) - \Phi_2^-(0)$ is a close approximation for $\Phi(0) = 2/3 = 0.6666 \dots$.

B Equality of Modified Beta Function and Shapley Value Weights

LEMMA 3. *We have the following recurrence relationship:*

$$\beta_{n,0} = \beta_{n,n} = \frac{1}{n+1} \text{ and } \beta_{n,m} = \frac{m}{n-(m-1)} \beta_{n,m-1}.$$

PROOF. There are two cases.

Case 1 (m is equal to zero, or n). We have the following integration.

$$\beta_{n,0} = \int_0^1 (1-x)^n dx = -\frac{(1-x)^{n+1}}{n+1} \Big|_0^1 = \frac{1}{n+1}.$$

A nearly identical calculation can be used to show $\beta_{n,n}$ is equal to $\frac{1}{n+1}$.

Case 2 ($0 < m < n$). We have the following partial integration:

$$\begin{aligned} \beta_{n,m} &= \int_0^1 x^m (1-x)^{n-m} dx \\ &= \frac{x^m (1-x)^{n-(m-1)}}{n-(m-1)} \Big|_0^1 - \int_0^1 \frac{-m}{n-(m-1)} x^{m-1} (1-x)^{n-(m-1)} dx \\ &= 0 + \frac{m}{n-(m-1)} \int_0^1 x^{m-1} (1-x)^{n-(m-1)} dx \\ &= \frac{m}{n-(m-1)} \beta_{n,m-1}. \end{aligned}$$

■

THEOREM 6. *The beta function $\beta_{n,m}$ is equal to the Shapley weight function $\gamma(n, m)$, with $0 \leq m \leq n$ and $m, n \in \mathbb{N}$.*

PROOF. The proof is by induction on m .

Base case ($m = 0$). According to Case 1 of Lemma 3, we have that $\beta_{n,0}$ is equal to $\frac{1}{n+1}$, which is equal to $\gamma(n, 0)$.

Inductive step ($m > 0$). Suppose $\beta_{n,k}$ is equal to $\gamma(n, k)$, $k \in \mathbb{N}$, we need to show $\beta_{n,k+1} = \gamma(n, k+1)$, $0 \leq k < n$. According to Case 2 of Lemma 3, $\beta_{n,k+1}$ is equal to $\frac{k+1}{n-k} \beta_{n,k}$. Using the inductive hypothesis, the latter is equivalent to

$$\frac{k+1}{n-k} \gamma(n, k) = \frac{k+1}{n-k} \cdot \frac{k!(n-k)!}{(n+1)!}$$

which matches the definition of $\gamma(n, k+1)$.

■

C Riemann Sum Samples

LEMMA 4. *$t'_\ell(k)$ is in range $[t_\ell(k), t_\ell(k+1)]$.*

PROOF. Recall the definition for $t_\ell(k) = \sin^2(\pi(k/2^{\ell+1}))$. Since $t'_\ell(k) = t_{\ell+1}(2k+1)$, we have that,

$$t'_\ell(k) = \sin^2\left(\pi \frac{k+1/2}{2^{\ell+1}}\right) = t'_\ell(k+1/2).$$

Since $k \in \{0, \dots, 2^\ell - 1\}$, $t_\ell(x)$ is increasing for $x \in [k, k+1]$ for all k . Therefore, since $k+1/2 \in [k, k+1]$, the result holds.

■

D Complexity and Error Analysis

D.1 Error - Step 1. It is important to assess the error and complexity of Step 1 of the Section 5 algorithm.

DEFINITION 9 (DARBOUX SUMS). Darboux sums [23, page 270] takes a partition $P = (z_0, z_1, \dots, z_r)$ of an interval $[a, b]$, where $a = z_0 < z_1 < \dots < z_r = b$, and a function f which maps (a, b) to \mathbb{R} . Each interval $[z_i, z_{i+1}]$ is called a subinterval. Let

$$M_i = \sup_{x \in [z_i, z_{i+1}]} f(x), \quad \text{and}$$

$$m_i = \inf_{x \in [z_i, z_{i+1}]} f(x), \quad i = 0, \dots, r-1.$$

The upper Darboux sum and the lower Darboux sum are:

$$U(f, P) = \sum_{i=0}^{r-1} M_i(z_{i+1} - z_i), \quad L(f, P) = \sum_{i=0}^{r-1} m_i(z_{i+1} - z_i).$$

COROLLARY 2. Given a partition $P = (z_0, \dots, z_r)$ of an interval $[a, b]$ and an integrable function $f: [a, b] \rightarrow \mathbb{R}$, any Riemann sum (Definition 7) is greater than or equal to the lower Darboux sum and less than or equal to the upper Darboux sum,

$$L(f, P) \leq \sum_{i=0}^{r-1} f(z'_i)(z_{i+1} - z_i) \leq U(f, P)$$

where $z'_i \in [z_i, z_{i+1}]$.

LEMMA 5. Given a partition $P = (z_0, \dots, z_r)$ of an interval $[a, b]$ and an integrable function $f: [a, b] \rightarrow \mathbb{R}$, the integral of f from a to b is greater than the lower Darboux sum and smaller than the upper Darboux sum.

$$L(f, P) \leq \int_a^b f(x) dx \leq U(f, P).$$

PROOF. By the Mean Value Theorem [23, page 233], there exists an $p_i \in [z_i, z_{i+1}]$, such that,

$$f(p_i) = \frac{1}{z_{i+1} - z_i} \int_{z_i}^{z_{i+1}} f(t) dt.$$

Hence, we can create the following Riemann sum (Definition 7),

$$\sum_{k=0}^{r-1} (z_{k+1} - z_k) f(p_k) = \sum_{k=0}^{r-1} \int_{z_k}^{z_{k+1}} f(x) dx = \int_a^b f(x) dx.$$

Thus, by Corollary 2, the result holds. ■

LEMMA 6. Let $P = (z_0, \dots, z_r)$ be a partition of an interval $[a, b]$ and suppose the function $f: [a, b] \rightarrow \mathbb{R}$ is integrable. Then, the error of a Riemann sum is bounded by the difference of the upper and lower Darboux sums, that is, the difference between the Riemann sum and the integral is bounded by,

$$\left| \int_a^b f(x) dx - \sum_{k=0}^{r-1} f(z'_k)(z_{k+1} - z_k) \right| \leq U(f, P) - L(f, P)$$

where $z'_k \in [z_k, z_{k+1}]$.

PROOF. We must show that the absolute difference between any given Riemann sum and the integral from a to b is less than or equal to the absolute difference between the upper and lower Darboux sums. Without loss of generality, suppose the integral is greater than the Riemann sum. By Lemma 5,

$$\int_a^b f(x)dx - \sum_{k=0}^{r-1} f(z'_k)(z_{k+1} - z_k) \leq U(f, P) - \sum_{k=0}^{r-1} f(z'_k)(z_{k+1} - z_k).$$

Similarly, by Corollary 2,

$$U(f, P) - \sum_{k=0}^{r-1} f(z'_k)(z_{k+1} - z_k) \leq U(f, P) - L(f, P).$$

■

Lemma 6 allows us to bound the error of any Riemann sum approximation for an integral, giving us a sequence of boxes that bound the error for their respective subinterval. A convenient result of our method is that given only a partition; we can guarantee error bounds given any selection of samples.

COROLLARY 3. Recall the function $b_{n,m}(x) = x^m(1-x)^{n-m}$ (Definition 6) and partition $P_\ell = (t_\ell(0), \dots, t_\ell(2^\ell))$ of $[0, 1]$. Lemma 6 implies that the error of a Riemann sum using $b_{n,m}$ and P_ℓ is upper bounded by,

$$\sum_{k=0}^{2^\ell-1} w_\ell(k)(M_k - m_k).$$

$w_\ell(k)$ is defined in Equation (19) and m_k, M_k are defined in Definition 9.

It is important to find a simple upper bound for the function $w_\ell(k)$ and the difference $M_k - m_k$.

LEMMA 7. $w_\ell(k)$ is upper bounded by a function that depends solely on ℓ :

$$w_\ell(k) \leq \frac{\pi}{2^{\ell+1}}.$$

PROOF. Recall Equation (19), $w_\ell(k) = \sin^2(a+b) - \sin^2(a)$, where $a = \pi k/2^{\ell+1}$, $b = \pi/2^{\ell+1}$. Then, we have,

$$w_\ell(k) = [\sin(a+b) + \sin(a)][\sin(a+b) - \sin(a)].$$

Proceeding with common trigonometric identities yields,

$$w_\ell(k) = \left[2 \sin \frac{b}{2} \cos \frac{b}{2} \right] \left[2 \sin \frac{2a+b}{2} \cos \frac{2a+b}{2} \right],$$

which is equal to,

$$\sin(b) \sin(2a+b).$$

Since $0 \leq \sin(2a+b) \leq 1$, and $\sin x \leq x$ when x is non-negative, the result holds.

■

REMARK 2. It is helpful to note that $b_{n,m}(x) = b_{n,n-m}(1-x)$.

LEMMA 8. Let $n \in \mathbb{N}$, and suppose $m \in \{1, \dots, n-1\}$, then the derivative of $b_{n,m}(x)$ is,

$$\frac{db_{n,m}(x)}{dx} = \frac{(m-nx)b_{n,m}(x)}{x(1-x)}.$$

PROOF. Recall the definition of $b_{n,m}(x) = x^m(1-x)^{n-m}$, then by the product rule,

$$\frac{db_{n,m}(x)}{dx} = mx^{m-1}(1-x)^{n-m} - (n-m)x^m(1-x)^{n-m-1}.$$

Pulling out the common terms yields,

$$x^{m-1}(1-x)^{n-m-1} (m(1-x) - (n-m)x).$$

Collecting like terms and rearranging gives,

$$\frac{(m-nx)(x^m(1-x)^{n-m})}{x(1-x)}.$$

■

LEMMA 9. For $m = 0, n$, the derivatives of $b_{n,m}$ are,

$$\frac{db_{n,0}(x)}{dx} = n(1-x)^{n-1} \quad \text{and} \quad \frac{db_{n,n}(x)}{dx} = nx^{n-1},$$

respectively.

LEMMA 10. Let $n \in \mathbb{N}$ and $m \in \{0, \dots, n\}$, then for all x in $[0, 1]$,

$$b_{n,m}(x) \leq b_{n,m}(m/n).$$

PROOF. Suppose $m = n$, then $b_{n,m}(x) = x^n$. Clearly, x^n is increasing on the interval $[0, 1]$, thus $b_{n,m}$ is maximized at $x = 1 = m/n$. By Remark 2, if $m = 0$, the max of $b_{n,m}$ is also 1 and this occurs at $x = 0 = m/n$.

Finally, if $1 \leq m \leq n-1$, then $b_{n,m}(0) = b_{n,m}(1) = 0$. Note that $b_{n,m}(x)$ is strictly positive for $x \in (0, 1)$, and there is only one critical point on that interval. Thus, the maximum must be the critical point x between $(0, 1)$. By Lemma 8, this critical point satisfies $m - nx = 0$. Therefore, $b_{n,m}(x)$ is maximized when $x = m/n$. ■

COROLLARY 4. If $x < m/n$, then $b_{n,m}(x)$ is increasing at x ,

$$\frac{db_{n,m}(x)}{dx} > 0,$$

and if $x > m/n$, then $b_{n,m}(x)$ is decreasing at x ,

$$\frac{db_{n,m}(x)}{dx} < 0.$$

DEFINITION 10 (NOTATION). We define the function $\gamma_\ell(n, m)$ as the following Riemann sum approximation for $\gamma(n, m)$,

$$\gamma_\ell(n, m) = \sum_{k=0}^{2^\ell-1} w_\ell(k) \cdot b_{n,m}(t'_\ell(k)).$$

Let $u_\ell(n, m)$ be the signed difference between $\gamma_\ell(n, m)$ and $\gamma(n, m)$,

$$u_\ell(n, m) = \gamma_\ell(n, m) - \gamma(n, m).$$

LEMMA 11. The estimation $\gamma_\ell(n, m)$ has an absolute error upper bounded by,

$$|u_\ell(n, m)| \leq \frac{\pi}{2^\ell} b_{n,m}(m/n).$$

PROOF. Note, for the sake of space, we omit the cases where $m = 0$ and $m = 1$, though they do follow the same bound. Suppose $m \in \{1, \dots, n-1\}$. By Corollary 3, we have,

$$|u_\ell(n, m)| \leq \sum_{k=0}^{2^\ell-1} w_\ell(k)(M_k - m_k).$$

Applying Lemma 7 shows this is less than or equal to,

$$\frac{\pi}{2^{\ell+1}} \sum_{k=0}^{2^\ell-1} M_k - m_k.$$

Define j_k, J_k to be in interval $[t_\ell(k), t_\ell(k+1)]$ such that $m_k = b_{n,m}(j_k)$, $M_k = b_{n,m}(J_k)$. Then,

$$\frac{\pi}{2^{\ell+1}} \sum_{k=0}^{2^\ell-1} M_k - m_k = \frac{\pi}{2^{\ell+1}} \sum_{k=0}^{2^\ell-1} b_{n,m}(J_k) - b_{n,m}(j_k).$$

For any k such that $t_\ell(k+1) \leq m/n$, by Corollary 4, $x \in (t_\ell(k), t_\ell(k+1))$ implies that $\frac{d}{dx} b_{n,m}(x)$ is strictly positive. Thus, the leftmost part of the subinterval $[t_\ell(k), t_\ell(k+1)]$ is the minimum with respect to $b_{n,m}(x)$ and the rightmost part is the maximum, so,

$$b_{n,m}(J_k) - b_{n,m}(j_k) = b_{n,m}(t_\ell(k+1)) - b_{n,m}(t_\ell(k)). \quad (26)$$

Similarly, for k such that $t_\ell(k) \geq m/n$, by Corollary 4, $x \in (t_\ell(k), t_\ell(k+1))$ implies $\frac{d}{dx} b_{n,m}(x)$ is strictly negative, so,

$$b_{n,m}(J_k) - b_{n,m}(j_k) = -[b_{n,m}(t_\ell(k+1)) - b_{n,m}(t_\ell(k))]. \quad (27)$$

If for some k , $t_\ell(k)$ is equal to m/n , then we have described each interval. Supposing that for all k , $t_\ell(k) \neq m/n$, there exists one other subinterval $[t_\ell(s), t_\ell(s+1)]$ that is non-monotonic. Its absolute error is bounded by,

$$b_{n,m}(J_s) - b_{n,m}(j_s) = \max_{r \in \{0,1\}} b_{n,m}(m/n) - b_{n,m}(t_\ell(s+r)). \quad (28)$$

Thus, we have the following upper bound for the absolute error,

$$\frac{\pi}{2^{\ell+1}} \left(\sum_{k=0}^{s-1} (M_k - m_k) + (M_s - m_s) + \sum_{k=s+1}^{2^\ell-1} (M_k - m_k) \right),$$

where we take $s = 0$ when there is no non-monotonic sub-interval. Plugging in Equations (26), 27, and 28, yields the absolute error upper bound of,

$$\max_{r \in \{0,1\}} \frac{\pi}{2^{\ell+1}} \left[\left(\sum_{k=0}^{s-1} b_{n,m}(t_\ell(k+1)) - b_{n,m}(t_\ell(k)) \right) + (b_{n,m}(m/n) - b_{n,m}(t_\ell(s+r))) - \left(\sum_{k=s+1}^{2^\ell-1} b_{n,m}(t_\ell(k+1)) - b_{n,m}(t_\ell(k)) \right) \right].$$

We can telescope both series into,

$$\max_{r \in \{0,1\}} \frac{\pi}{2^{\ell+1}} \left[(b_{n,m}(t_\ell(s)) - b_{n,m}(0)) + (b_{n,m}(m/n) - b_{n,m}(t_\ell(s+r))) - (b_{n,m}(t_\ell(2^\ell)) - b_{n,m}(t_\ell(s+1))) \right].$$

Note that $b_{n,m}(0) = b_{n,m}(2^\ell) = 0$, and that $-b_{n,m}(t_\ell(s+r))$ cancel out either $b_{n,m}(s)$ or $b_{n,m}(s+1)$. The above equation is upper bounded by,

$$\max_{r \in \{0,1\}} \frac{\pi}{2^{\ell+1}} (b_{n,m}(m/n) + b_{n,m}(t_\ell(s+r))).$$

Thus, Lemma 10 implies the result. ■

LEMMA 12. Let n be greater or equal to two and suppose m is in $\{1, \dots, n-1\}$, we have the following inequality,

$$\binom{n}{m} \cdot b_{n,m}(m/n) < \frac{1}{\sqrt{2\pi}} \cdot \sqrt{\frac{n}{m(n-m)}}.$$

PROOF. First note that $b_{n,m}(m/n)$ can be rewritten as,

$$\frac{m^m (n-m)^{n-m}}{n^n}. \quad (29)$$

Additionally, by a slightly improved version of Stirling's approximation [45], for k greater than or equal to one,

$$\sqrt{2\pi k} \left(\frac{k}{e}\right)^k e^{\frac{1}{12k+1}} < k! < \sqrt{2\pi k} \left(\frac{k}{e}\right)^k e^{\frac{1}{12k}}. \quad (30)$$

It follows directly from Equation (30), and the inequality $(12n)^{-1} - (12m+1)^{-1} - (12(n-m)+1)^{-1} < 0$, that,

$$\binom{n}{m} = \frac{n!}{m!(n-m)!} < \frac{1}{\sqrt{2\pi}} \cdot \sqrt{\frac{n}{m(n-m)}} \cdot \frac{n^n}{m^m (n-m)^{n-m}}. \quad (31)$$

Multiplying the Equations (29) and (31) yields the result. \blacksquare

DEFINITION 11. We write a Shapley value estimation using γ_ℓ as,

$$\Phi_\ell(i) = \sum_{S \subseteq F \setminus \{i\}} \gamma_\ell(|S|, |F \setminus \{i\}|) \cdot (V(S \cup \{i\}) - V(S)).$$

LEMMA 13. The following inequality holds for n greater or equal to three,

$$\sum_{m=1}^{n-1} \binom{n}{m} b_{n,m}(m/n) \leq \sqrt{\frac{\pi n}{2}}.$$

PROOF. The bound for odd n is similar to finding a bound for an even n . We proceed assuming n is equal to $2k+1$ where $k \in \mathbb{N}$. By Lemma 12, we immediately get the upper bound,

$$\sqrt{\frac{n}{2\pi}} \sum_{m=1}^{2k} \frac{1}{\sqrt{m(n-m)}}.$$

This can be rewritten as,

$$\sqrt{\frac{n}{2\pi}} \left[\left(\sum_{m=1}^{k-1} \frac{1}{\sqrt{m(n-m)}} \right) + \left(\frac{1}{\sqrt{k(n-k)}} \right) + \left(\sum_{m=k+1}^{2k} \frac{1}{\sqrt{m(n-m)}} \right) \right].$$

The expansions of the summations are equal. We have the upper bound,

$$\sqrt{\frac{2n}{\pi}} \left(\frac{1}{2\sqrt{k(n-k)}} + \sum_{m=1}^{k-1} \frac{1}{\sqrt{m(n-m)}} \right). \quad (32)$$

Next, note that $1/\sqrt{m(2k-m)}$ is a decreasing function on the interval $(0, n/2]$. So,

$$\frac{1}{2\sqrt{k(n-k)}} + \sum_{m=1}^k \frac{1}{\sqrt{m(2k-m)}}, \quad (33)$$

can be interpreted as the lower Darboux sum of function $(m(n-m))^{-1/2}$, on the interval $(0, k]$, using partition $P = (0, 1, \dots, k-1, k, k+1/2)$.

By Lemma 5, this implies Equation (33) is upper bounded by,

$$\int_0^{n/2} \frac{1}{\sqrt{x(n-x)}} dx.$$

By converting the product $x(n-x)$ to vertex form, performing a substitution, and finally performing a trigonometric substitution, we find the definite integral equals $\pi/2$. Combining this with Equation (32) shows the result. ■

THEOREM 7. *If n is greater or equal to two, assuming Steps 2 and 3 introduce no error, the Shapley value estimation has the following upper bound on absolute error,*

$$|\Phi_\ell(i) - \Phi(i)| \leq \frac{(V_{\max} - V_{\min})\sqrt{n}}{2^{\ell-3}}. \quad (34)$$

PROOF. By Definitions 10 and 11, the ℓ th Shapley value approximation can be written as,

$$\Phi_\ell(i) = \sum_{S \subseteq F \setminus \{i\}} [\gamma(|S|, |F \setminus \{i\}|) + u_\ell(|S|, |F \setminus \{i\}|)] \cdot [V(S \cup \{i\}) - V(S)].$$

Pulling the terms apart and applying the standard equation for Shapley values give,

$$\Phi_\ell(i) = \Phi(i) + \sum_{S \subseteq F \setminus \{i\}} u_\ell(|S|, |F \setminus \{i\}|) \cdot (V(S \cup \{i\}) - V(S)).$$

Thus, the Shapley estimation absolute error is equal to,

$$|\Phi_\ell(i) - \Phi(i)| = \left| \sum_{S \subseteq F \setminus \{i\}} u_\ell(|S|, |F \setminus \{i\}|) \cdot (V(S \cup \{i\}) - V(S)) \right|$$

which is thus upper bounded by,

$$\sum_{S \subseteq F \setminus \{i\}} |u_\ell(|S|, |F \setminus \{i\}|)| \cdot |V(S \cup \{i\}) - V(S)|.$$

Recall V_{\max} and V_{\min} , defined in Equations (6) and (7). This gives a new upper bounds for $|\Phi_\ell(i) - \Phi(i)|$,

$$(V_{\max} - V_{\min}) \cdot \sum_{S \subseteq F \setminus \{i\}} |u_\ell(|S|, |F \setminus \{i\}|)|.$$

By Lemma 11 and a reinterpretation of the sum, we have the upper bound,

$$\frac{\pi(V_{\max} - V_{\min})}{2^\ell} \cdot \sum_{m=0}^n \binom{n}{m} b_{n,m}(m/n).$$

For n equal to two, the sum is less than $(V_{\max} - V_{\min})/2^{\ell-3}$. Hence, the result holds. Assuming n greater or equal to three, by Lemma 13, the above is less than,

$$\frac{\pi(V_{\max} - V_{\min})}{2^\ell} \left(\sqrt{\frac{\pi n}{2}} + \binom{n}{0} 1 + \binom{n}{n} 1 \right) = \frac{\pi(V_{\max} - V_{\min})}{2^\ell} \left(\sqrt{\frac{\pi n}{2}} + 2 \right).$$

Hence, the result holds. ■

D.2 Error - Step 2. Suppose U_V^\pm is an imperfect implementation of \hat{V}^\pm , such that,

$$\delta_h^\pm = \langle V^\pm(h) | 1 \rangle \langle 1 | V^\pm(h) \rangle - \hat{V}^\pm(h), \quad \delta_h = \delta_h^+ - \delta_h^- \quad (35)$$

where $|V^\pm(h)\rangle = U_V^\pm(h) |0\rangle$ (Equation (14)). We also define,

$$\delta_{\max} \geq \max_{h \in \{0, \dots, 2^n - 1\}} |\delta_h|. \quad (36)$$

In plain language, δ_h is the error of our quantum implementation in how much player i would contribute to the coalition represented by the binary string h . Additionally, δ_{\max} upper bounds the error of δ_h .

With these definitions in mind, let us see how the error in our quantum implementation propagates. Let us first recall our state after Step 2 (Section 5).

$$\text{tr}_{\text{Pt}, \text{P1}} (|\psi_2^\pm\rangle\langle\psi_2^\pm|) = \sum_{m=0}^n \sum_{h \in H_m} \left(\sum_{k=0}^{2^\ell-1} w_\ell(k) b_{n,m}(t'_\ell(k)) \right) \cdot |V^\pm(h)\rangle_{\text{Ut}} \langle V^\pm(h)|_{\text{Ut}}.$$

By Definition 10, this is equal to,

$$\sum_{m=0}^n \sum_{h \in H_m} (\gamma(n, m) + u_\ell(n, m)) |V^\pm(h)\rangle_{\text{Ut}} \langle V^\pm(h)|_{\text{Ut}}.$$

We are interested in the expected value of the Ut register, which is equal to,

$$\langle \psi_2^\pm | (I^{\otimes \ell+n} \otimes |1\rangle\langle 1|) | \psi_2^\pm \rangle = \sum_{m=0}^n \sum_{h \in H_m} (\gamma(n, m) + u_\ell(n, m)) \langle V^\pm(h) | 1 \rangle \langle 1 | V^\pm(h) \rangle.$$

By Equation (35), this is equivalent to,

$$\sum_{m=0}^n \sum_{h \in H_m} (\gamma(n, m) + u_\ell(n, m)) (\hat{V}^\pm(h) + \delta_h^\pm).$$

Subtracting our estimates for Φ_i^- from Φ_i^+ and multiplying by $V_{\max} - V_{\min}$ results in,

$$(V_{\max} - V_{\min}) \left(\sum_{m=0}^n \sum_{h \in H_m} (\gamma(n, m) + u_\ell(n, m)) \left((\hat{V}^+(h) - \hat{V}^-(h)) + \delta_h \right) \right).$$

Multiplying the terms out yields,

$$\Phi_i + (V_{\max} - V_{\min}) \left(\sum_{m=0}^n \sum_{h \in H_m} [\gamma(n, m) \delta_h] + \sum_{m=0}^n \sum_{h \in H_m} [u_\ell(n, m) (\hat{V}^+(h) - \hat{V}^-(h))] + \sum_{m=0}^n \sum_{h \in H_m} [u_\ell(n, m) \delta_h] \right).$$

Thus, we have three error terms, and we now find an absolute bound for each of them. The first term can be bounded easily, using Lemma 1 and Equation (35), we have the following,

$$\left| \sum_{m=0}^n \sum_{h \in H_m} \gamma(n, m) \delta_h \right| \leq \sum_{m=0}^n \sum_{h \in H_m} \gamma(n, m) |\delta_h| \leq \delta_{\max} \sum_{m=0}^n \sum_{h \in H_m} \gamma(n, m) = \delta_{\max}.$$

The second term is calculated in Theorem 7. In particular, noting that we have $\hat{V}^\pm(h) \in [0, 1]$,

$$\left| \sum_{m=0}^n \sum_{h \in H_m} u_\ell(n, m) (\hat{V}^+(h) - \hat{V}^-(h)) \right| \leq \frac{\sqrt{n}}{2^{\ell-3}}.$$

Finally, we have the error introduced by the third term. By an almost identical calculation to that in Theorem 7, we find that,

$$\left| \sum_{m=0}^n \sum_{h \in H_m} u_\ell(n, m) \delta_h \right| \leq \frac{\delta_{\max} \sqrt{n}}{2^{\ell-3}}.$$

Thus, the combined error introduced from Steps 1 and 2 is bounded by:

$$(V_{\max} - V_{\min}) \cdot \left(\frac{\sqrt{n}}{2^{\ell-3}} \delta_{\max} + \frac{\sqrt{n}}{2^{\ell-3}} + \delta_{\max} \right). \quad (37)$$

Note that, no matter how large we make ℓ , the error persists if we are unable to also minimize δ_{\max} .

D.3 Error - Step 3. For this step, we use a quantum subroutine for speeding up Monte Carlo Methods [22]. With a probability greater than $8/\pi^2$, the procedure succeeds. The process can be repeated $O(\log(1/p))$ times to improve the success probability to $1 - p$. Suppose we perform t iterations of amplitude estimation. If we are trying to extract value μ , and the result is $\tilde{\mu}$, the error is bounded,

$$|\tilde{\mu} - \mu| \leq 2\pi \frac{\sqrt{\mu(1-\mu)}}{t} + \frac{\pi^2}{t^2}.$$

In our case, $\mu = (\Phi_i - V_{\min}) / (V_{\max} - V_{\min}) \in [0, 1]$, so we can take the following more simple upper bound,

$$|\tilde{\mu} - \mu| \leq 2\pi \frac{t\sqrt{\mu} + \pi}{t^2}.$$

Since we are extracting the value $\mu = (V_{\max} - V_{\min}) \langle \psi_2 | (I^{\otimes \ell+n} \otimes |1\rangle\langle 1|) | \psi_2 \rangle$, our final error is,

$$(V_{\max} - V_{\min}) \left(\frac{\sqrt{n}}{2^{\ell-3}} \delta_{\max} + \frac{\sqrt{n}}{2^{\ell-3}} + \delta_{\max} + 2\pi \frac{t\sqrt{\mu} + \pi}{t^2} \right).$$

D.4 Complexity. Suppose we want a total error of ϵ . This section finds an upper bound of complexity given a desired error. Let $\sqrt{n}/2^{\ell-3}, \delta_{\max}, 2\pi(t\sqrt{\mu} + \pi)/t^2 \leq \epsilon'$ be less than or equal to 1, then the error is bounded by,

$$(V_{\max} - V_{\min}) \left((\epsilon')^2 + 3\epsilon' \right) \leq 4(V_{\max} - V_{\min}) \epsilon'.$$

Hence, an upper bound of error ϵ can be achieved if, $\epsilon' \leq \epsilon / (4(V_{\max} - V_{\min}))$.

For notational simplicity, we define,

$$\lambda = \frac{V_{\max} - V_{\min}}{\epsilon}. \quad (38)$$

to get $\sqrt{n}/2^{\ell-3}$ less than ϵ' , a partition register of size,

$$\ell = \lceil \log_2(\lambda \sqrt{n}) \rceil + 5, \quad (39)$$

is sufficient.

Recall $C_D(\ell)$ to be the complexity of implementing D_ℓ (cf. Definition 8) with an error with respect to $w_\ell(k)$ of less than $4^{-\ell}$. δ_{\max} on the other hand depends on the complexity of computing U_V^\pm with max error ϵ' , which we write $C_V(\epsilon')$.

DEFINITION 12. We denote the complexity to implement U_V^\pm , such that the maximum error δ_{\max} (Equations (35) and (36)) is upper bounded by ϵ' , as $C_V(\epsilon')$.

Additionally, to sufficiently bound the error introduced by Step 3, we must satisfy $2\pi(t\sqrt{\mu} + \pi)/t^2 \leq \epsilon / (4(V_{\max} - V_{\min}))$. Suppose that we wish our absolute error ϵ to be less than the difference $\Phi_i - V_{\min}$. Using the quadratic formula, we see

it is sufficient to take t equal to,

$$t = \left\lceil \frac{28\sqrt{(\Phi_i - V_{\min})(V_{\max} - V_{\min})}}{\epsilon} \right\rceil. \quad (40)$$

Finally, with the upper bounds for these important factors in mind, let us consider the complexity in terms of CNOT gates given these upper bounds. Generating $|\psi_{1a}\rangle$ is complexity $C_D(\ell)$. Next, evolving to $|\psi_{1b}\rangle$ takes $n\ell$ controlled rotations, which can be implemented with $2n\ell$ CNOTs in $2 \cdot \max(n, \ell)$ layers. From here, producing state $|\psi_2\rangle$ has complexity $C_V(4^{-1}\lambda^{-1})$. Next, Step 3 involves amplitude estimation, meaning the above steps are repeated t times, followed by an Inverse Quantum Fourier Transform on $\log_2(t)$ bits taking $O(\log_2^2 t)$ operation. Hence, the total complexity is bounded by,

$$t \cdot \left(C_D(\ell) + 2n\ell + C_V\left(\frac{1}{4\lambda}\right) \right) + O(\log^2 t), \quad (41)$$

where λ is defined in Equation (38), and conservative values for ℓ and t are given in Equations (39) and 40 respectively.

THEOREM 8. *Suppose there exists a constant real positive number b such that $C_V(a\epsilon) > (b/a)C_V(\epsilon)$ for all real positive a . The total complexity of the algorithm is,*

$$O\left(\frac{\sqrt{(\Phi_i - V_{\min})(V_{\max} - V_{\min})}}{\epsilon} \left(C_D(\log_2(\lambda\sqrt{n})) + n \log_2(\lambda\sqrt{n}) + C_V\left(\frac{1}{4\lambda}\right) \right)\right).$$

PROOF. The result follows directly from Equation (41). ■